



Article

Investigating the Properties of ABS-Based Plastic Composites Manufactured by Composite Plastic Manufacturing

Raghunath Bhaskar ^{1,*} , Javaid Butt ² and Hassan Shirvani ²

¹ Transporter Engineering Limited, Transporter House, Unit 4-7 Gosfield Business Park, The Old Airfield, Halstead CO9 1SA, UK

² School of Engineering and Built Environment, Faculty of Science and Engineering, Anglia Ruskin University, Chelmsford CM1 1SQ, UK

* Correspondence: raghub@transporter-eng.co.uk

Abstract: Additive manufacturing (AM) technologies have revolutionized the manufacturing sector due to their benefits, such as design flexibility, ease of operation, and wide material selection. The use of AM in composites production has also become quite popular to leverage these benefits and produce products with customized properties. In this context, thermoplastic materials are widely used in the development of plastic-based composites due to their affordability and availability. In this work, composite plastic manufacturing (CPM) has been used to manufacture plastic-based composites with bespoke properties in a cost- and time-effective manner. Various plastic-based composites have been manufactured using CPM by interlacing acrylonitrile butadiene styrene (ABS) with thermally activated materials. Three different thermally activated materials (graphene–carbon hybrid paste, heat cure epoxy, and graphene epoxy paste) have been used in this work to produce plastic-based composites. Thermally activated materials that are commercially available include graphene–carbon hybrid paste and heat cure epoxy. The graphene epoxy paste was a concoction made by incorporating three different weight percentages of graphene nanoplatelets (0.2 wt.%, 0.4 wt.%, and 0.6 wt.%) with heat cure epoxy. The composites were manufactured with multiple layers of thermally activated materials at different intervals to investigate their effect. The parts were manufactured and tested according to British and international standards. Experimental tests of mass, dimensions, ultrasonics, tensile strength, hardness, and flexural strength were conducted to evaluate the properties of composites manufactured by CPM. The parts manufactured by CPM showed superior mechanical properties compared to commercially available ABS. The increase was shown to be in the range of 8.1% to 33% for tensile strength, 17.8% to 30.2% for hardness, and 6.2% to 24.4% for flexural strength, based on the composite configurations. The results demonstrate that the CPM process can produce high-quality plastic composites and can be used to create products with customized properties in a time-effective manner.

Keywords: additive manufacturing; thermoplastics; ABS plastic; thermally activated materials; composite plastic manufacturing; plastic-based composites; ultrasonic test; tensile test; hardness; flexural test



Citation: Bhaskar, R.; Butt, J.; Shirvani, H. Investigating the Properties of ABS-Based Plastic Composites Manufactured by Composite Plastic Manufacturing. *J. Manuf. Mater. Process.* **2022**, *6*, 163. <https://doi.org/10.3390/jmmp6060163>

Academic Editor: Joshua M. Pearce

Received: 31 October 2022

Accepted: 12 December 2022

Published: 17 December 2022

Publisher's Note: MDPI stays neutral with regard to jurisdictional claims in published maps and institutional affiliations.



Copyright: © 2022 by the authors. Licensee MDPI, Basel, Switzerland. This article is an open access article distributed under the terms and conditions of the Creative Commons Attribution (CC BY) license (<https://creativecommons.org/licenses/by/4.0/>).

1. Introduction

Additive manufacturing (AM) has been widely used to equip multiple materials for composites development and has gained significant attention in recent years [1–3]. Fused filament fabrication (FFF) or fused deposition modeling (FDM—trademark of Stratasys) is a commercially available AM process that employs thermoplastic materials for manufacturing [4–7]. The two most popular and widely used thermoplastics for the FFF process are polylactic acid (PLA) and acrylonitrile butadiene styrene (ABS). PLA is a semi-crystalline polymer with evenly packed molecules and is biodegradable. ABS is an amorphous polymer made up of non-uniform molecules [8–11]. Thermoplastic

materials are widely available in various forms (filaments, pellets, granules) and are used for a wide range of applications in the manufacturing sector [12,13]. FFF parts are heavily influenced by process parameters such as printing/bed/nozzle temperature, infill pattern/percentage, print speed, etc. PLA and ABS are thermoplastic materials commonly used by researchers in process optimization and to manufacture plastic composites via FFF. Researchers have investigated the effects of material extrusion rates, extrusion temperatures, line width, and layer height for FFF manufactured parts. Optimization of process parameters results in better properties for FFF manufactured parts but is a time- and resource-intensive task [14–18].

Due to its ease of operation and software/hardware modifications, FFF has also been widely used for composites manufacturing. Various materials have been developed over the years to leverage the ease of operation offered by FFF by incorporating nano additives, metal powders, and graphene nanoplatelets to manufacture FFF filaments [19–24]. PLA and ABS have been interlaced with copper mesh and glass fiber sheets using hybrid fused deposition modeling (HFDM) to manufacture plastic-based composites with bespoke mechanical properties [25–27]. PLA and ABS thermoplastics have also been interlaced with graphene nanoplatelets (GNPs), graphene oxide (GO), and carbon nanotubes (CNTs) to manufacture graphene-based filament materials. However, interlacing thermoplastics with nanomaterials requires a number of pre-treatment techniques with a long lead time before a filament can be manufactured and used for functional purposes [28–31]. Furthermore, epoxy and graphene paste have also been incorporated with thermoplastics for composite manufacturing as they are widely used to bond plastic parts together and are popular due to their properties and ease of use. These materials are thermally activated and cured under specified time and temperature conditions [32–34].

To leverage the benefits of FFF, Tambrallimath et al. [28] developed a polymer nanocomposite filament to manufacture parts via FDM. The composite filaments were developed by combining (melt blend) polycarbonate (PC) and ABS with GNPs in various proportions (0.2 wt.%, 0.4 wt.%, 0.6 wt.%, and 0.8 wt.%). Several preprocessing techniques were used, such as drying the PC and ABS pellets for 4 h to remove moisture before compounding them together at different temperatures to obtain a composite filament, thus resulting in a longer lead time. Dul et al. [29] developed an ABS-graphene nanocomposite filament by compounding ABS pellets with 4 wt.% graphene nanoplatelets. The process was carried out in three batches for each composition and then followed by granulation. The compounded materials were then hot pressed at 190 °C to obtain square plaques. After the compression molding, the samples were manufactured with various build orientations using FDM. The materials were blended (compression molding) to form a filament for fabrication (filament extrusion), which is a time-consuming process. Similarly, Vidakis et al. [30] investigated the mechanical properties of 3D printed ABS graphene and carbon nanocomposites. Two nano additive materials (GNPs and CNTs) were interlaced with ABS. Graphene nanoplatelets were mixed with ABS in four concentrations (0.5 wt.%, 2.5 wt.%, 5 wt.%, and 10 wt.%) and fabricated via extrusion melting at various temperatures. The addition of GNPs to the ABS matrix decreased the tensile strength for all the composition when compared to pure ABS. This could be due to agglomeration and percolation threshold formation in the obtained composite filament [35–39]. Furthermore, the reduction indicates weakening bonding between the graphene nanoplatelets and polymer matrix. The process involves several preprocessing techniques and resources to obtain composite filament, which is a time-consuming process. Aumnate et al. [31] developed a composite filament by incorporating graphene-based materials into polymer to enhance mechanical, thermal, and electrical properties. The composite filament was obtained by combining ABS and graphene oxide (GO) using dry and solvent mixing methods to fabricate using the FFF process. Graphene oxide was prepared using Hummer's method and then a solution was made using dimethylformamide (DMF). The GO/DMF dispersion was mixed with ABS/DMF solution and then sonicated for 2 h. After the sonication process, the mixture was dried to obtain the composite filament (20 wt.% GO in ABS). The composite filament (ABS/GO)

was compounded together in the twin screw extrusion to obtain filament materials. To achieve the composite filament, several preprocessing techniques were used. Furthermore, the obtained ABS/GO composite filament made using the dry mixing method failed to print due to the agglomeration of GO within the ABS, resulting in nozzle clogging and jamming issues.

It is to be noted that the mechanical properties of FFF manufactured parts can be enhanced through postprocessing operations such as annealing, sanding, polishing, and epoxy coating. However, post-treatment processes require more time and resources, and there is still uncertainty in achieving consistent properties for intended applications [40–42]. Annealing is one of the most common post-processes for FFF parts because of the nature of the FFF process and the prevalence of voids, air gaps, and cracks in these parts. The process of annealing helps in minimizing these defects and relieving internal stresses to improve mechanical strength. The dimensional tolerances (shrinkage and expansion) of the manufactured parts could also be impacted by the time-consuming and labor-intensive process of annealing [43–45]. Several researchers have used annealing to improve the properties of FFF-printed thermoplastics. Butt and Bhaskar [45] investigated the effects of annealing on the mechanical properties of FFF-printed thermoplastics at different temperatures. They used polymeric materials (PLA and ABS) and metal-infused thermoplastics, i.e., copper-enhanced PLA (Cu-PLA) and aluminum-enhanced ASA (acrylonitrile styrene acrylate) in their work. The samples were annealed for one hour and cooled for two hours inside a convection oven. The annealed samples were investigated using dimensional analysis, ultrasonic testing, tensile testing, microstructural analysis, and hardness testing. The results showed that annealing adversely affects the dimensional tolerances of FFF manufactured parts. Therefore, it is essential to take shrinkage and the expansion into consideration if parts are to be annealed.

All the aforementioned methods demonstrate the capabilities and limitations of FFF/FDM in terms of manufacturing plastic-based composites with bespoke properties. It is also evident from the literature that the existing manufacturing methods are associated with multiple limitations including long curing times, and pre- and posttreatment requirements; these result in longer lead times to make the desired product. Furthermore, the commercially available composite materials in filament, pellets, or paste form can be compounded together in a filament extrusion machine to obtain composite filaments. However, such processes are time-consuming and involve subprocesses within the production, which results in high costs. Composite plastic manufacturing (CPM) is a new additive manufacturing process that reduces the limitations of separate filament production, long curing times, pre- and postprocesses, thus resulting in a faster lead time. The process has been explained in detail in our previous work [46] where PLA was interlaced with thermally activated materials. The results showed the capabilities of the CPM process and its effectiveness in manufacturing high-quality plastic composites. This paper focuses on the effect of adding multiple layers of thermally activated materials to ABS to investigate the behavior of plastic—thermally activated materials bonding. The next section (Section 2) explains the methodology used in this study. Section 3 provides the discussion of experimental results, and conclusions of this work are outlined in Section 4.

2. Methodology

2.1. Materials and Manufacturing Process

The composite plastic manufacturing (CPM) process has been used in this work to manufacture ABS-based plastic composites. CPM integrates two material extrusion additive manufacturing technologies (i.e., fused filament fabrication and syringe extrusion) in a desktop-based system, as shown in Figure 1. The working principle of the CPM process has been discussed in detail in our previous work [46].

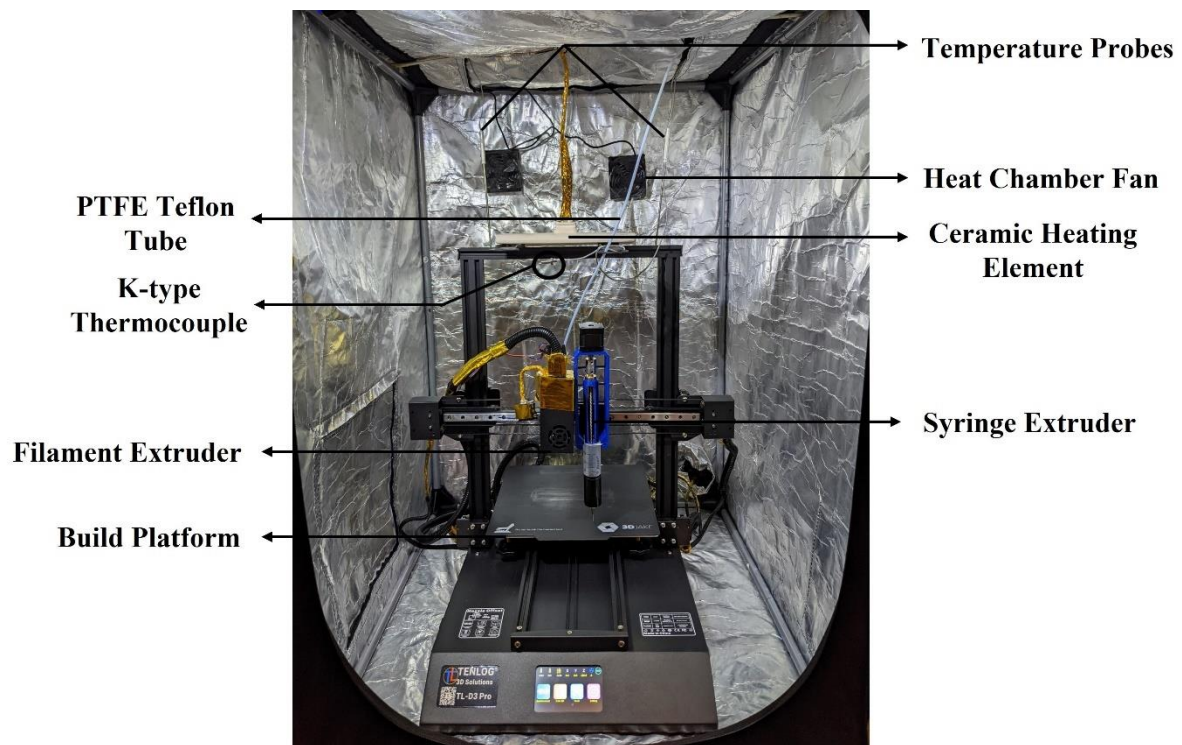


Figure 1. Composite plastic manufacturing process [46].

The system was designed and developed with two independent extruders working together with one depositing polymer material and the other depositing thermally activated material. There was no requirement for tool head change as the system already had two independent extruders to dispense multiple materials (both filament-based and thermally activated materials). The system was equipped with a heat chamber that cured the thermally activated materials during the process and eliminated the pre- and postprocess requirements. The system activated the heating chamber once the process was turned on and functioned according to the defined temperature. If the process value was less than the set value, the temperature controller displayed the inside temperature, at which point the heating element activated. If the temperature remained constant, the heating element was turned off automatically via the proportional-integral-derivative (PID) controller.

The CPM process starts with a 3D CAD model (stl format) of the part, which is sliced into cross-sections using the slicing software Ultimaker Cura to determine the number of layers based on the geometry of the part before being transferred to the machine for manufacturing. Cura allows users to easily modify g-codes and it offers options for a number of useful settings, such as pause at height or layer, which are features that are helpful for this work. The CAD file was built up with pauses so that thermally activated material could deposit on ABS plastic at different layer numbers.

The operation starts with printing support material that can be removed after the completion of the build. After the completion of the support material, the system prints the build material in a layer-by-layer configuration based on the part's geometry. The filament extruder deposits polymer material whereas the syringe extruder dispenses thermally activated material. The layer of thermally activated material is programmed for set intervals (depending on the number of layers), after which the system pauses the filament extruder head and moves it to the home position. The system then activates the syringe extruder to deposit the thermally activated material. The heating chamber turns on at a specific temperature (determined by the material being used) following the deposition of the thermally activated material to cure the deposited material. This is done to make sure that the thermally activated material cures during the printing process, reducing the amount of time and postprocessing steps required for the production of

plastic-based composites. The heat applied to the parts during the process helps in reducing internal stresses and achieving strong bonding. The system monitors layer completion after each layer before switching to the other extruder. If a layer is incomplete, the system prints the additional material needed to finish the layer and reach the desired layer thickness. The build material is printed by the system until it reaches the geometry's specified total number of layers (N). The part can be removed and tested in accordance with the user's needs when the build is finished.

In this work, ABS was interlaced with different thermally activated materials to manufacture plastic composites using the CPM process and to investigate the behavior of plastic-thermally activated materials bonding for multiple layers. Filamentum ABS Extrafill [47] was purchased from 3D FilaPrint, Southend-on-Sea, UK and this material will be referred to as ABS. From here onwards, the thermally activated materials will be referred to as TA materials. The TA materials interlaced with ABS were graphene-carbon hybrid paste (Dycotec Materials, Swindon, UK) [48], which will be referred to as GCHP, and heat cure epoxy ES566 (Permabond Engineering Adhesives Ltd., Hampshire, UK) [49], which will be referred to as HCE. The graphene-carbon hybrid paste (GCHP) from Dycotec Materials had a viscosity of 2500–6500 cP and the recommended print speed was 70 mm/s. The print speed was kept at 30 mm/s for all the TA materials to maintain good consistency of the rate of deposition and accuracy. Heat cure epoxy (HCE) ES566 from Permabond® is a single-part epoxy with a viscosity of 60,000–120,000 cP at 20 rpm, which can withstand high temperatures for longer periods. Furthermore, graphene nanoplatelets (referred to as GNPs) [50] in powder form (Nanografi Nano Technology, Ankara, Turkey) were used to create graphene epoxy paste (referred to, asGEP). The GNPs from Nanaografi had a 30 µm diameter, and 5 nm thickness with 99.9 + % purity.

2.2. Process Parameters and Configuration of Composites

For the material characterization, tensile test samples, hardness samples, and three-point flexural testing, samples were manufactured according to BS EN ISO 527-2: 2012 [51], BS EN ISO 868:2003 [52], and BS EN ISO 178:2019 [53], respectively. ABS samples were manufactured using the traditional FFF process and the plastic-based composites were manufactured using the CPM process. The samples were manufactured in flat orientation and the dimensions of the samples are shown in Figure 2.

The 3D CAD model (stl format) of the part was sliced into cross-sections using slicing software called Ultimaker Cura 5.2.1 [54]. The parameters for nozzle, build platform, and heat chamber were set according to the technical datasheets of the materials. The system automatically activated the heat chamber to cure the TA material. The heat transfer occurred through the convection process, where the heat rose upward and circulated in the chamber due to the fan. The heat chamber was kept at ambient temperature for ABS and upon depositing the TA material, the heating element turned on and started to heat up the chamber. The heat chamber temperature was kept at 100 °C for all the plastic-based composites. The system was programmed to pause at set intervals, after which the filament extruder moved back to the home position. The syringe extruder then moved to the exact coordinates to a print single layer of TA material on ABS plastic. The thermally activated material was added to ABS without any surface treatment and a total of five samples were manufactured and tested for each material configuration [46].

Graphene-carbon hybrid paste (GCHP) was used to manufacture ABS/GCHP composites. Heat cure epoxy ES566 (HCE) was used to manufacture ABS/HCE composites. HCE and GNPs were used to manufacture ABS/GEP composites with three different wt.% of GNPs (0.2, 0.4, and 0.6). The HCE was used to manufacture ABS/HCE as well as ABS/GEP composites. GNPs were manually mixed for 5 s at room temperature after being pre-weighed before being added to HCE. For homogenous dispersion, the mixture was then sonicated with an Ultrasonic Homogenizer Sonicator Cell Disruptor (Vevor, UK) [55]. The mixture was sonicated for 60 min at 80% output power and 20 kHz frequency [56–58]. The homogeneous GEP was carefully loaded into the syringe extruder after sonication

for composite manufacturing. Table 1 shows the process parameters for ABS and plastic composites manufactured by CPM. The parts were built at two different print speed; i.e., ABS at a speed of 60 mm/s and TA material at 30 mm/s. The layer thickness was set to 0.2 mm with 100% infill pattern of ‘lines’. The nozzle temperature for ABS was kept at 240 °C and the TA material was printed at 0 °C with the build plate temperature kept at 80 °C for all the samples.

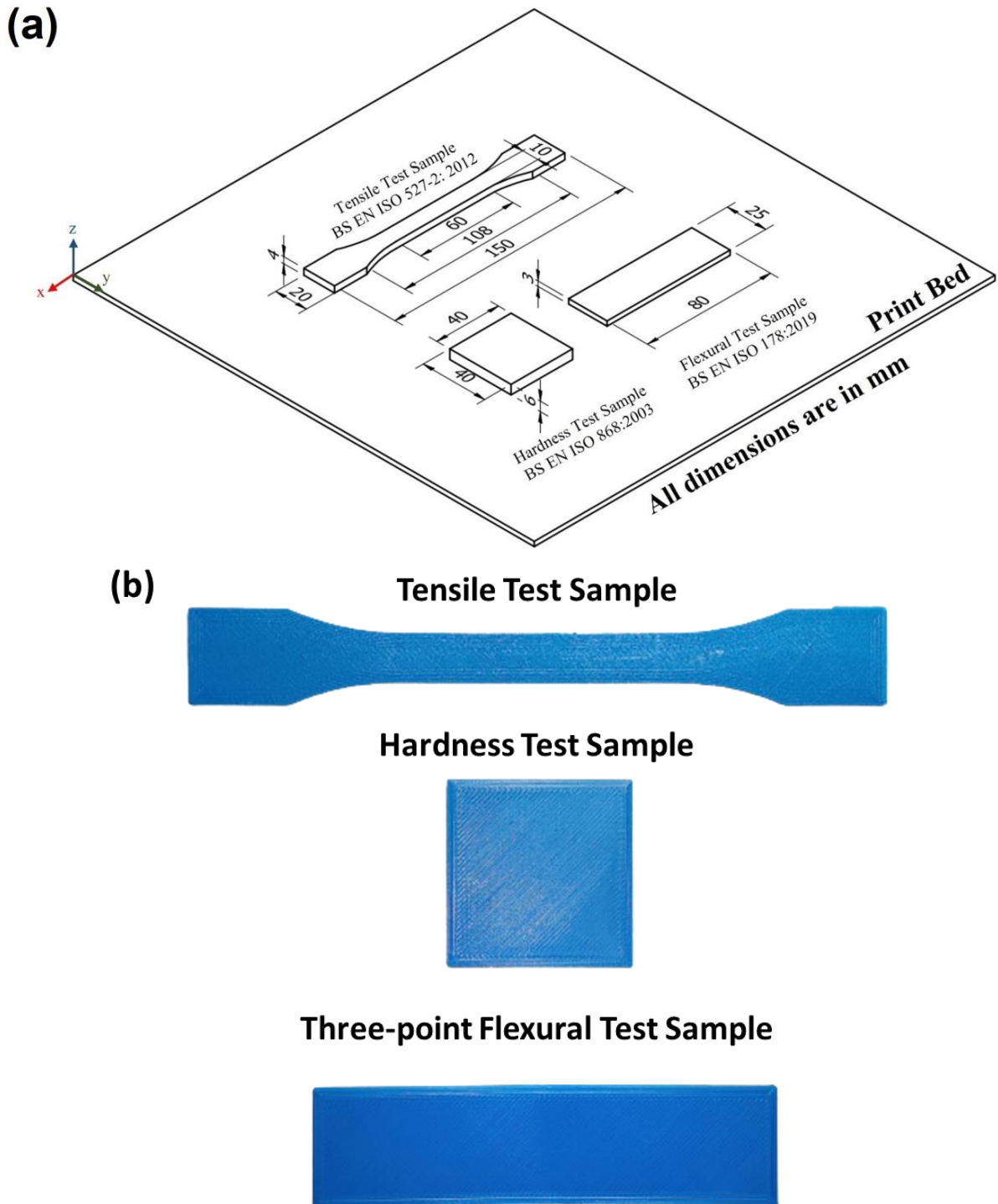


Figure 2. Manufacture of samples: (a) dimensions and build orientation; (b) tensile, hardness and three-point flexural testing samples.

Table 1. Process parameters for ABS and ABS-based plastic composites.

Samples	Extruder Temperature (°C)		Bed Temperature (°C)	Heat Chamber Temperature (°C)	Print Speed (mm/s)		Layer Thickness (mm)	
	Filament	Syringe			ABS	TA Material	ABS	TA Material
ABS ¹	240	N/A	80	0	60	N/A	0.2	N/A
ABS/GCHP ²	240	0	80	100	60	30	0.2	0.1
ABS/HCE ²	240	0	80	100	60	30	0.2	0.1
ABS/0.2 GEP ²	240	0	80	100	60	30	0.2	0.1
ABS/0.4 GEP ²	240	0	80	100	60	30	0.2	0.1
ABS/0.6 GEP ²	240	0	80	100	60	30	0.2	0.1

¹—Fused filament fabrication; ²—composite plastic manufacturing.

ABS was interlaced with the TA materials at different intervals for tensile, hardness, and flexural samples. Plastic composites were manufactured with increasing layers of thermally activated materials. Multiple layers of thermally activated materials were added to ABS after different polymer layers' completion to find the optimal number of TA material layers that could be added, because after this optimal number, the tensile and flexural strength started to deteriorate. For single-layered composites, TA material was added at 50% of the overall thickness of the sample and for a double-layered plastic composite, two TA material layers were deposited at 40% and 80%. A total of 5 layers of TA material were added to tensile samples (4 mm). For hardness samples, the composites were made with a single layer of TA materials added at different intervals of build (70%, 80%, and 90%). Research conducted by Butt et al. [27] on the development of Cu/PLA composites shows that the addition of foreign material closer to the surface of the sample is better in assessing its hardness characteristics due to the nature of the indentation test. A total of 3 layers of TA material were added to flexural samples (3 mm).

The total number of layers can be obtained from Ultimaker Cura during the slicing process. The layer thickness for ABS is kept at 0.2 mm; therefore, the total number of layers can be calculated by dividing the sample thickness by layer thickness. For a 4 mm tensile sample, the calculations were carried out = 4/0.2 = 20 (total number of sliced layers). The total number of sliced layers for hardness samples (40 mm × 40 mm × 6 mm) were 30 (6/0.2 = 30). For a 3 mm flexural sample, the total number of sliced layers was 15 (3/0.2 = 15).

The layer calculations were made using the following formula:

$$Relevant N^{th} layer number = \frac{total\ number\ of\ sliced\ layers}{total\ number\ of\ TA\ material\ layers + 1} \times n. \tag{1}$$

where n denotes the interval between $1 \leq n \leq total\ number\ of\ TA\ material\ layers$

$$Manufacturing\ completion = \frac{relevant\ N^{th}\ layer\ number}{total\ number\ of\ sliced\ layers} \times 100\% \tag{2}$$

Based on the above formula, the calculations were carried out for adding 1 layer of TA material to a 4 mm tensile sample.

$$Relevant\ N^{th}\ layer\ number = \frac{20}{1 + 1} \times 1 = 10. \tag{3}$$

$$Manufacturing\ completion = \frac{10}{20} \times 100\% = 50\% \tag{4}$$

For adding two TA material layers to a 4 mm tensile sample,

$$Relevant\ N^{th}\ layer\ number = \frac{20}{2 + 1} \times 1 = 6.6666 \sim 7\ for\ 1^{st}\ layer \tag{5}$$

$$\text{Manufacturing completion} = \frac{7}{20} \times 100\% = 35\% \tag{6}$$

$$\text{Relevant } N^{\text{th}} \text{ layer number} = \frac{20}{2+1} \times 2 = 13.3333 \sim 13 \text{ for } 2^{\text{nd}} \text{ layer} \tag{7}$$

$$\text{Manufacturing completion} = \frac{13}{20} \times 100\% = 65\% \tag{8}$$

The relevant layer numbers for TA material addition and manufacturing completion were calculated in this manner. Values such as 6.66 and 13.33 were rounded off to 7 and 13, respectively. The same calculations were carried out for all the test samples to manufacture plastic-based composites. Tables 2–4 show the configuration of adding multiple layers of TA materials for tensile testing samples, hardness testing samples, and flexural testing samples, respectively. Figure 3 shows the schematics of ABS/TA materials layout.

Table 2. Configuration of tensile testing samples.

Number of TA Material	Manufacturing Completion	Relevant Layer Number
1	50%	10
2	35%, 65%	7, 13
3	25%, 50% 75%	5, 10, 15
4	20%, 40%, 60%, 80%	4, 8, 12, 16

Table 3. Configuration of hardness testing samples.

Number of TA Material	Manufacturing Completion	Relevant Layer Number
1	70%	21
1	80%	24
1	90%	27

Table 4. Configuration of three-point flexural testing samples.

Number of TA Material	Manufacturing Completion	Relevant Layer Number
1	50%	7
2	40%, 80%	5, 10
3	25%, 50%, 75%	4, 7, 11

2.3. Measurements and Experimental Testing

An extensive comparative analysis was carried out on the plastic composites to establish the capability and effectiveness of the CPM process. The manufactured samples were tested based on two methods, i.e., destructive, and non-destructive. Both these testing methods are essential to understand the effectiveness and capabilities of the CPM process. Destructive testing (DT) methods are used to determine the exact failure point of a material or a component. On the other hand, non-destructive testing (NDT) methods also determine the object’s behavior without destroying the actual product [59–61]. The composites were manufactured by interlacing ABS with multiple layers of TA materials. The purpose of adding multiple layers is to determine the optimal number of layers that can be added to the overall thickness to improve mechanical strength. The heat chamber was set to activate whenever a TA material deposited a layer on a thermoplastic material. This allowed the TA material to cure during the printing process; thus, eliminating the need for post-processing for the manufactured composites. Research conducted by Butt and Bhaskar et. al [45] shows that the annealed parts can adversely affect the dimensional accuracy of FFF-printed parts (shrinkage or expansion) in any of the three axes (x, y, and z). In this context, mass measurement and dimensional analysis were carried out to analyze the effect of adding a 0.1 mm TA material layer to ABS. This was also done to investigate whether the presence

of the heat chamber affected the manufactured parts and to evaluate the tolerance value of CPM manufactured composites. Mass measurement and dimensional analysis were carried out on the dog-bone samples manufactured according to BS EN ISO 527-2:2012 [51]. Measurement of mass was conducted using a CBK 8H weighing scale (from Adam Equipment, UK) with a resolution of 0.1 g. The dimensions of the dog-bone samples were measured using a digital Vernier Calliper.

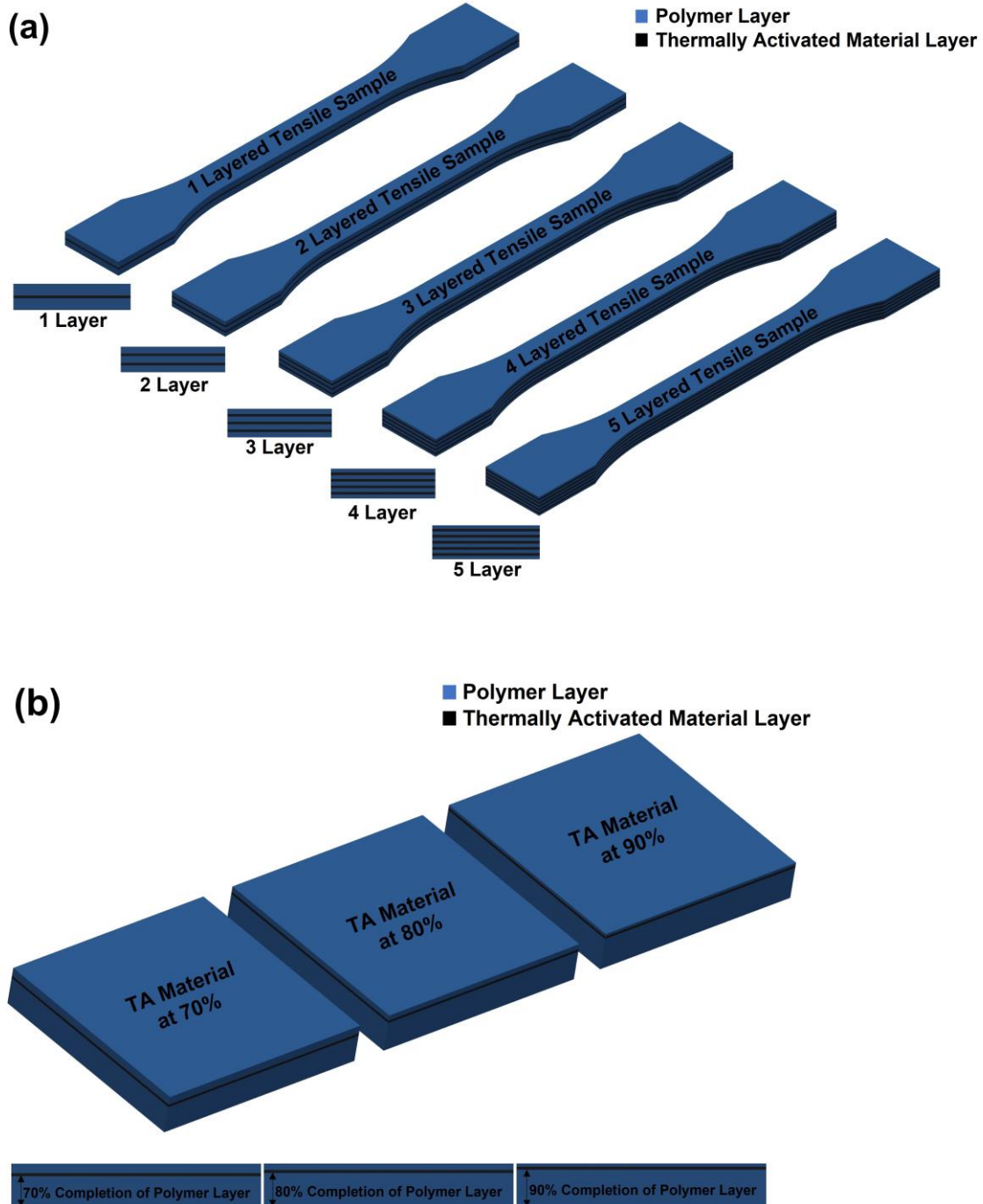


Figure 3. Cont.

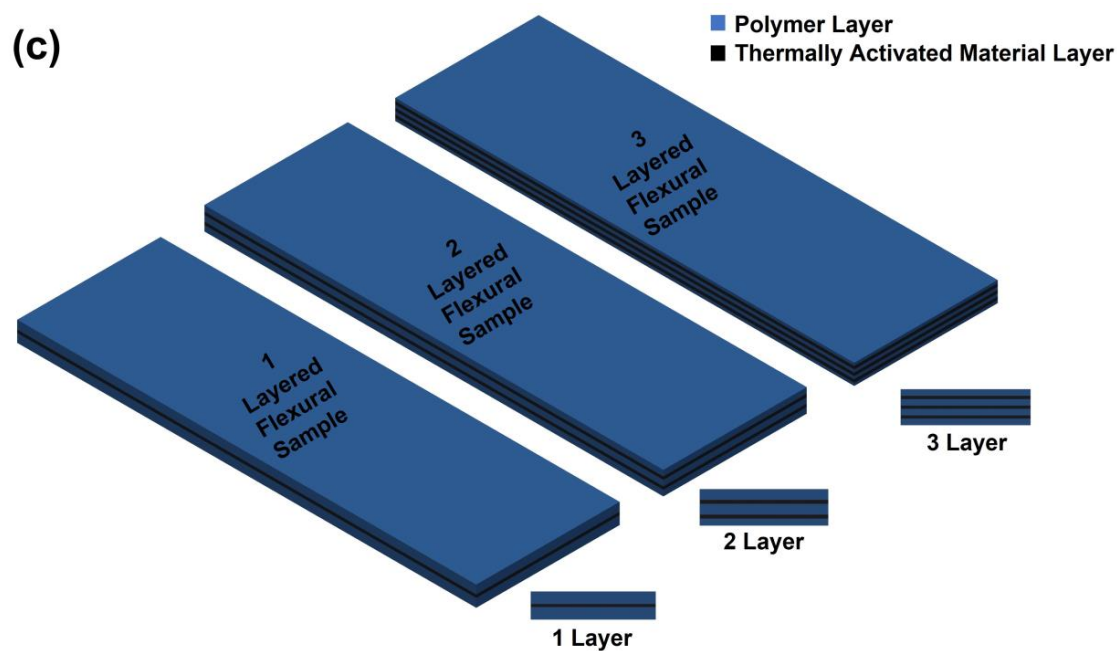


Figure 3. Schematics of ABS/TA materials layout: (a) tensile test samples; (b) hardness test samples; (c) three-point flexural test samples.

After the measurement of mass and dimensional analysis, ultrasonic testing (UT) was conducted on the manufactured samples to obtain the transmission time of sound waves. UT is a popular non-destructive (NDT) method because it allows assessment of materials (defects, cracks, and voids) without destruction [59–61]. UT was conducted using Proceq PUNDIT® PL-200 [62] comprising two transducers (54 kHz) and a measuring resolution of 0.1 μ s. Couplant gel was used to facilitate the transmission of ultrasonic sound waves through the samples. The manufactured parts were tested at three different points along their length to obtain an average value. The tensile test samples were manufactured and tested according to BS EN ISO 527-2:2012 [51] on a Universal Tensile Testing Machine (Hounsfield H50KM) with a load cell of 5 kN and a cross-head speed of 1.5 mm/s. The hardness samples were manufactured according to BS EN ISO 868:2003 [52] and values were measured on the Shore D Durometer [63]. The indentation was measured on five different points to determine the average hardness value for ABS and CPM plastic composites. The three-point flexural test samples were manufactured according to BS EN ISO 178:2019 [53] on a Universal Tensile Testing Machine with a speed of 2 mm/min. The diameter of the supports was 10 mm with a span length of 60 mm to support the specimens.

3. Experimental Results and Discussion

3.1. Measurement of Mass

The measurement of mass was the first analysis conducted on the samples to evaluate the effect of adding TA material to ABS. FFF-manufactured parts tend to show inaccuracy in their mass and dimensions. This is due to several factors, including printing/bed temperature, bed level, material flow rate, and print speed. Researchers have analyzed different optimization techniques during the slicing the process to enhance the accuracy of FFF-printed parts [15–18]. The actual mass was obtained from Cura during the slicing process. Cura showed a mass of 10 g for tensile samples, which was been kept as reference for the percentage difference calculation to analyze the results. The percentage differences were calculated for ABS and CPM plastic composites. The ABS sample showed a mass of 9.78 g whereas the expected value was 10 g. The calculation carried out was $((9.78 - 10)/10) \times 100 = -2.2\%$. The percentage differences were calculated using this relation for all the samples. Figure 4 shows the percentage differences for mass measurements. ABS samples were manufactured

using FFF, and it showed a difference of -2.2% from the actual mass (10 g). The composites manufactured using the CPM process did not show significant percentage differences when compared to ABS samples. The difference was observed to be within the tolerance value (-1.2 to -2%). It is evident from Figure 4 that single-layered composite showed relatively lower mass than the others. The mass of the samples started to increase after the addition of multiple layers of TA materials to ABS. For every single layer addition of TA material to ABS, the mass increased by 0.2 g. This can be observed in all the composites, where the highest mass was observed for five-layered composites with a percentage difference of -1.2% . The highest mass value of 9.88 g was observed for all the five-layered composites. The results show that the composites manufactured using the CPM process were within the tolerance range and did not exceed the actual mass. It is also evident that plastic composites showed accuracy in their mass, unlike FFF-manufactured parts. The same consistency was observed for all the composites manufactured by CPM, where the mass increased by 0.2 g for every layer addition.

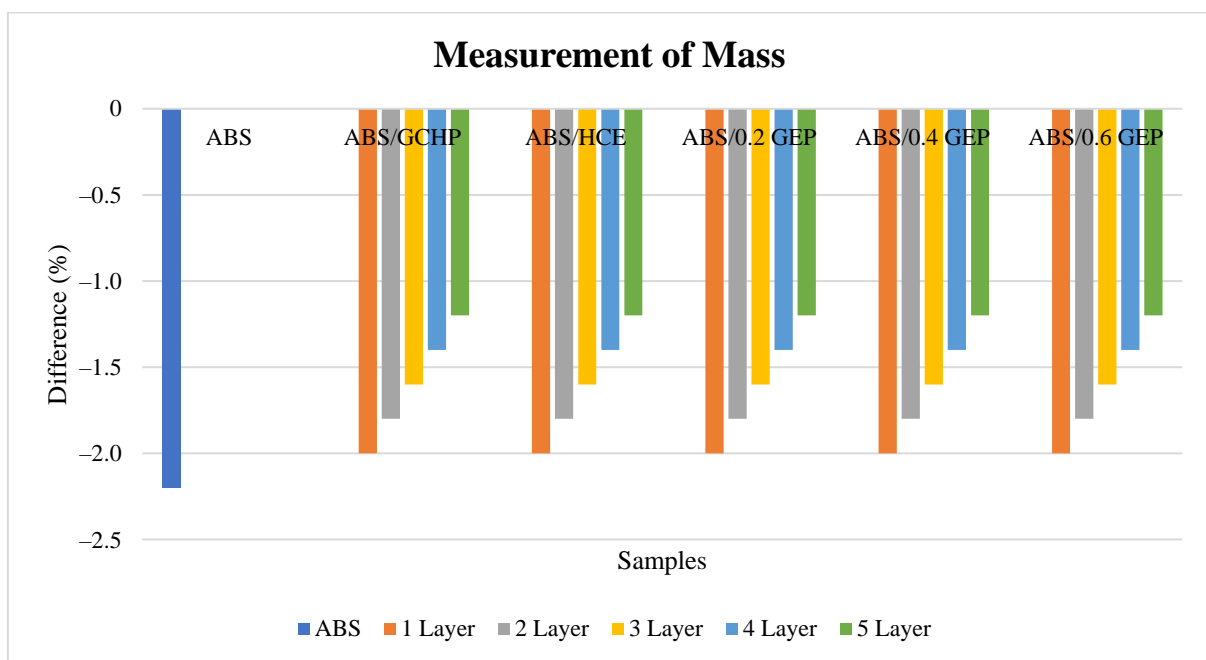


Figure 4. Percentage differences of mass measurements for ABS-based plastic composites.

The percentage difference was shown to be between -1.8% and -2% for single- and double-layered composites. All the single-layered composites showed a mass of 9.80 g. The 3-, 4-, and 5-layered composites showed increased mass but were within the tolerance range of actual mass. The double-layered composites showed a 0.4 g increase in their mass when compared to ABS. The 3- and 4-layered composites showed an increase of 0.6 g and 0.8 g in their mass. The results show that the parts manufactured by CPM were not adversely affected by the addition of TA material to ABS. It was also clear that addition of TA material to the ABS enhanced the accuracy of the overall mass. The mass of the desired part could be adjusted based on the product requirements, thus making the process versatile to produce bespoke parts with customised properties. It should also be noted that the composites demonstrated consistent mass for all the CPM-manufactured parts. This demonstrates the efficacy of the process, in which the parts are manufactured with greater precision than FFF and with bespoke properties.

3.2. Dimensional Analysis

Dimensional analysis on tensile samples was performed to investigate the tolerances of CPM-manufactured parts with commercially available ABS manufactured by FFF. Di-

dimensional analysis was conducted on the tensile samples. The dimensions of the tensile samples (150 mm × 20 mm × 4 mm) were measured using the Vernier Calliper. To analyze the results, the percentage differences along the X, Y, and Z axes were calculated. ABS showed a negative difference of −0.4% and −3% for X and Y axes. Testing of the percentage difference for ABS along the Z-axis was carried out as follows $((3.7 - 4)/4) \times 100 = -7.5\%$. The percentage differences were calculated in this manner for all three axes. Figure 5 shows the percentage differences for all three axes (X, Y, and Z) for all the samples.

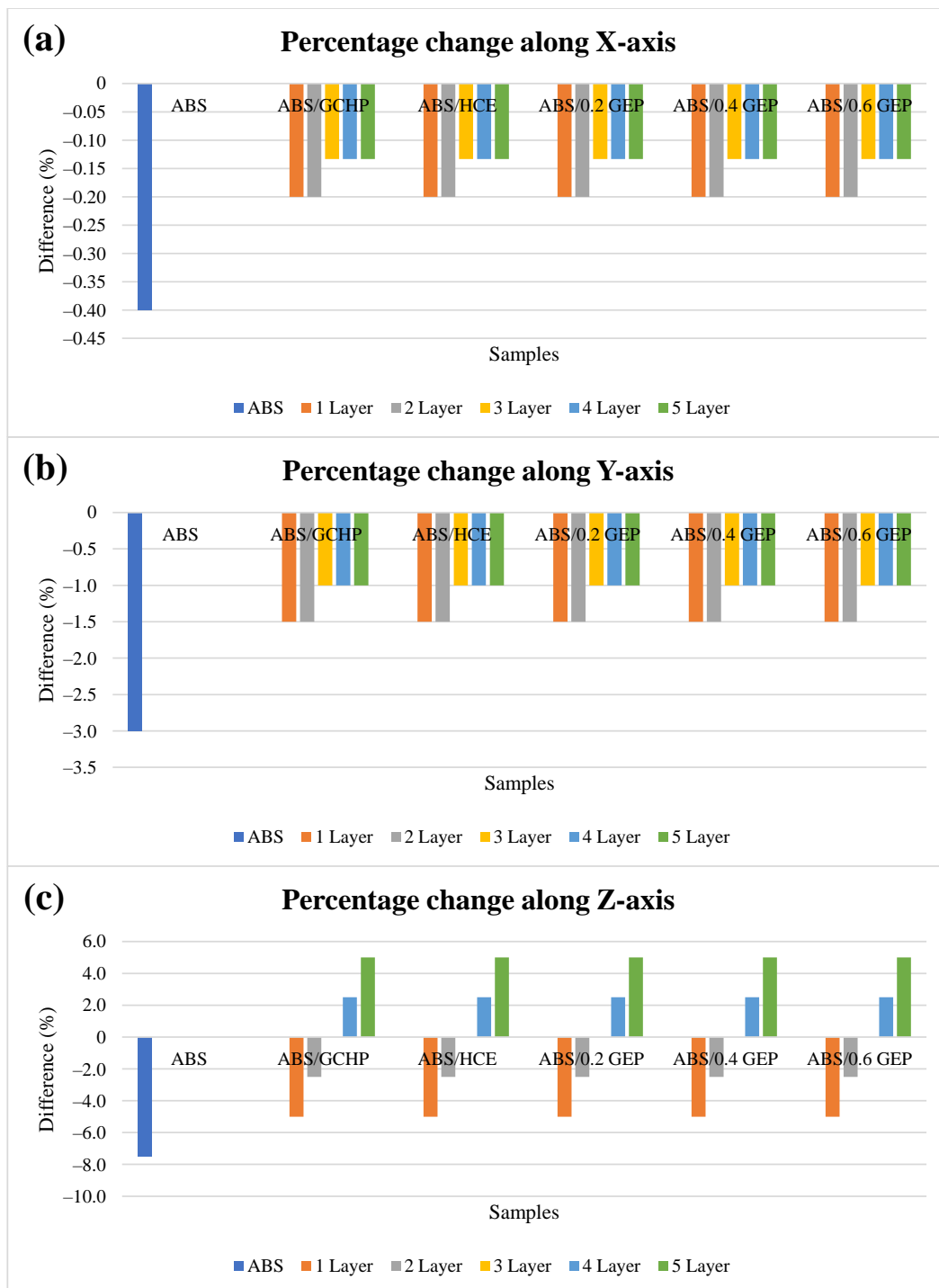


Figure 5. Dimensional analysis: (a) percentage change along X-axis; (b) percentage change along Y-axis; (c) percentage change along Z-axis.

The CPM plastic composites showed very minimal percentage differences along their X and Y axes when compared to ABS. The single- and double-layered plastic composites showed consistent values of -0.2% along their X-axis. For the 3-, 4-, and 5-layered composites, the accuracy increased with a difference of -0.13% along their X-axis, as shown in Figure 5a. A similar pattern was observed along the Y-axis, where the 1- and 2-layered composites showed consistent difference of -1.5% , whereas the 3-, 4-, and 5-layered composites showed -1% changes as shown in Figure 5b. ABS showed a percentage difference of -3% along the Y-axis. The measurement of Z-axis (thickness) was vital because the TA material was added to ABS in an incremental manner (multiple layers); therefore, it was essential to evaluate whether the addition increased the overall thickness of the samples. ABS showed a thickness of 3.7 mm with -7.5% difference along the Z-axis. The single-layered composites showed a percentage difference of -5% along their Z-axis for all the plastic composites manufactured with different thermally activated materials. A thickness increase of 0.1 mm was observed for each layered composite, as shown in Figure 5c.

All the single-layered composites showed a thickness of 3.8 mm with a percentage difference of -5% , whereas the double-layered composites showed -2.5% change along their Z-axis. The three-layered composites showed 100% accuracy in thickness (4 mm) value with 0% difference. A positive increase of 2.5% and 5% was observed for 4- and 5-layered composites, respectively. The highest increase was observed for five-layered composites, where the maximum thickness was 4.2 mm with a 5% increase. The results show that the parts can be manufactured in a consistent manner with minimal inaccuracies. An increase of 0.1 mm in total thickness was observed for 4- and 5-layered composites, whose tolerances can be taken into consideration by designers based on the product requirements. It should also be noted that the consistent addition of TA material improved the dimensional accuracy of the final product, which has been observed for three-layered composites (ABS/GCHP, ABS/HCE, ABS/0.2 GEP, ABS/0.4 GEP, and ABS/0.6 GEP). These results show that the CPM-manufactured parts were not adversely affected by the addition of TA materials and showed consistent results along the three axes.

3.3. Ultrasonic Testing

Researchers have demonstrated the effectiveness of ultrasonic testing in assessing defects in thermoplastic and composite products [15,26,45,46]. The purpose of UT is to determine whether the parts made by CPM have reduced internal stresses, air gaps/voids, and transmission time. As a non-destructive test, it helps to determine the compactness of the deposited layers, as well as the bond quality of the plastic and TA materials. The time taken by the sound waves to travel from one transducer to the other through the test piece was measured, and the results were plotted for comparison. ABS was interlaced with different thermally activated materials (GCHP, HCE, 0.2 wt.% GEP, 0.4 wt.% GEP, and 0.6 wt.% GEP) to manufacture plastic composites. The results show that the time taken for sound waves to travel through ABS was 2.3 μs . ABS/GCHP composites showed lower transmission times when compared to ABS and the results are shown in Figure 6. ABS/GCHP 1 and 2 samples showed a transmission time of 2.0 μs . The lowest transmission time of 1.9 μs was observed for ABS/GCHP three-layered composites. Both 4- and 5-layered ABS/GCHP composites showed a transmission time of 2.0 μs , respectively. The results clearly show that the addition of GCHP to ABS did not adversely affect the compactness of the deposited layers and helped in creating a more compact part with better layer adhesion.

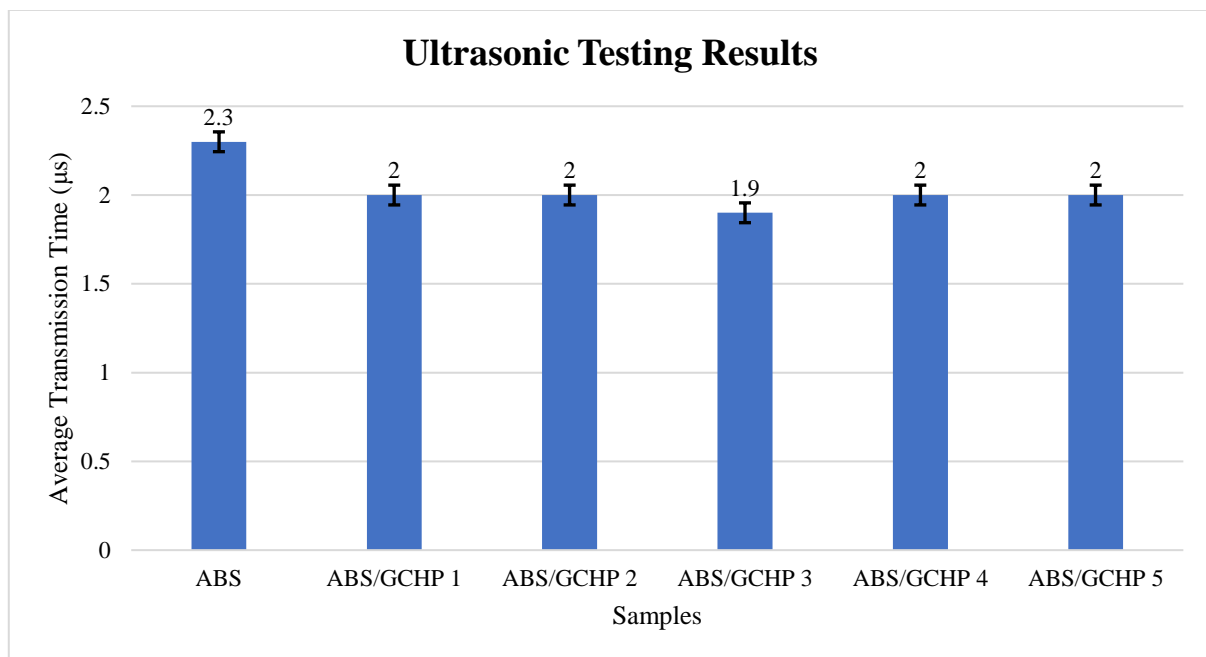


Figure 6. Ultrasonic testing results of ABS/GCHP composites with ABS.

On the other hand, ABS/HCE composites showed a consistent transmission time, as shown in Figure 7. The 1- and 2-layered composites showed transmission time of 2.0 μs. The lowest transmission time of 1.9 μs was observed for 3- and 4-layered samples. ABS/HCE 5 samples showed a transmission time of 2.0 μs, which was lower than that of ABS (2.3 μs).

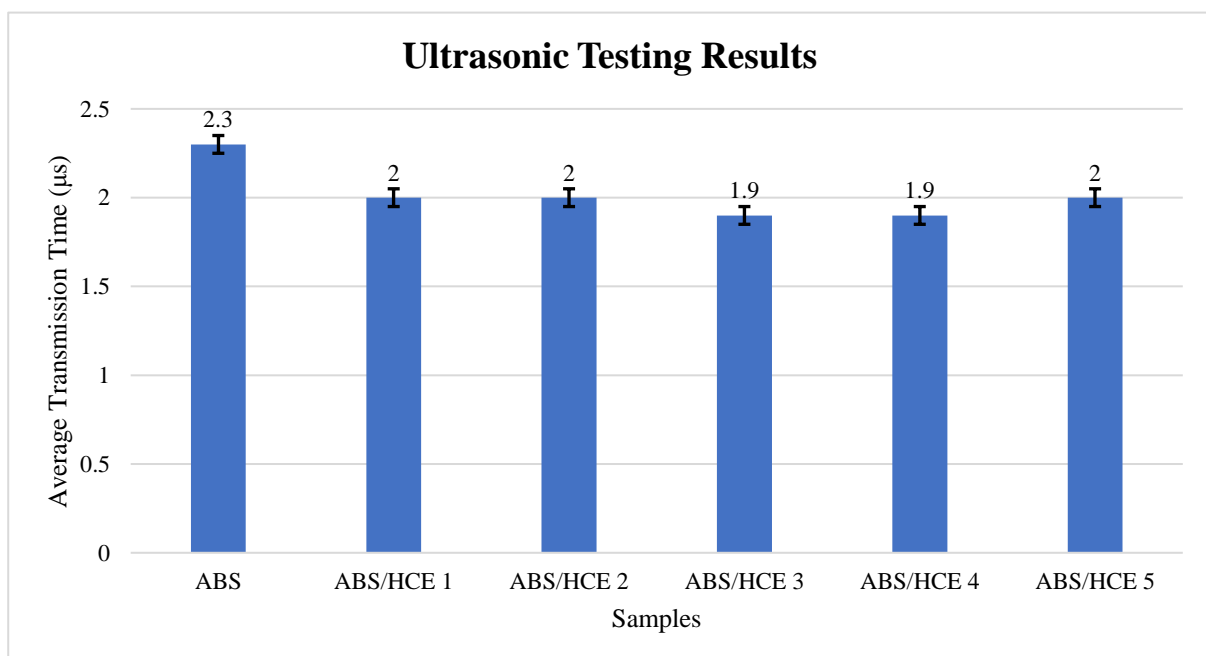


Figure 7. Ultrasonic testing results of ABS/HCE composites with ABS.

The GEP concoction was obtained by mixing HCE with three different weight percentages (0.2 wt.%, 0.4 wt.%, and 0.6 wt.%) of GNPs. The mixtures were ultrasonically processed to obtain a uniform homogeneous mixture, which improves the bonding between the polymer layer and the TA materials. The ultrasonic results for ABS/GEP composites with ABS are shown in Figure 8.

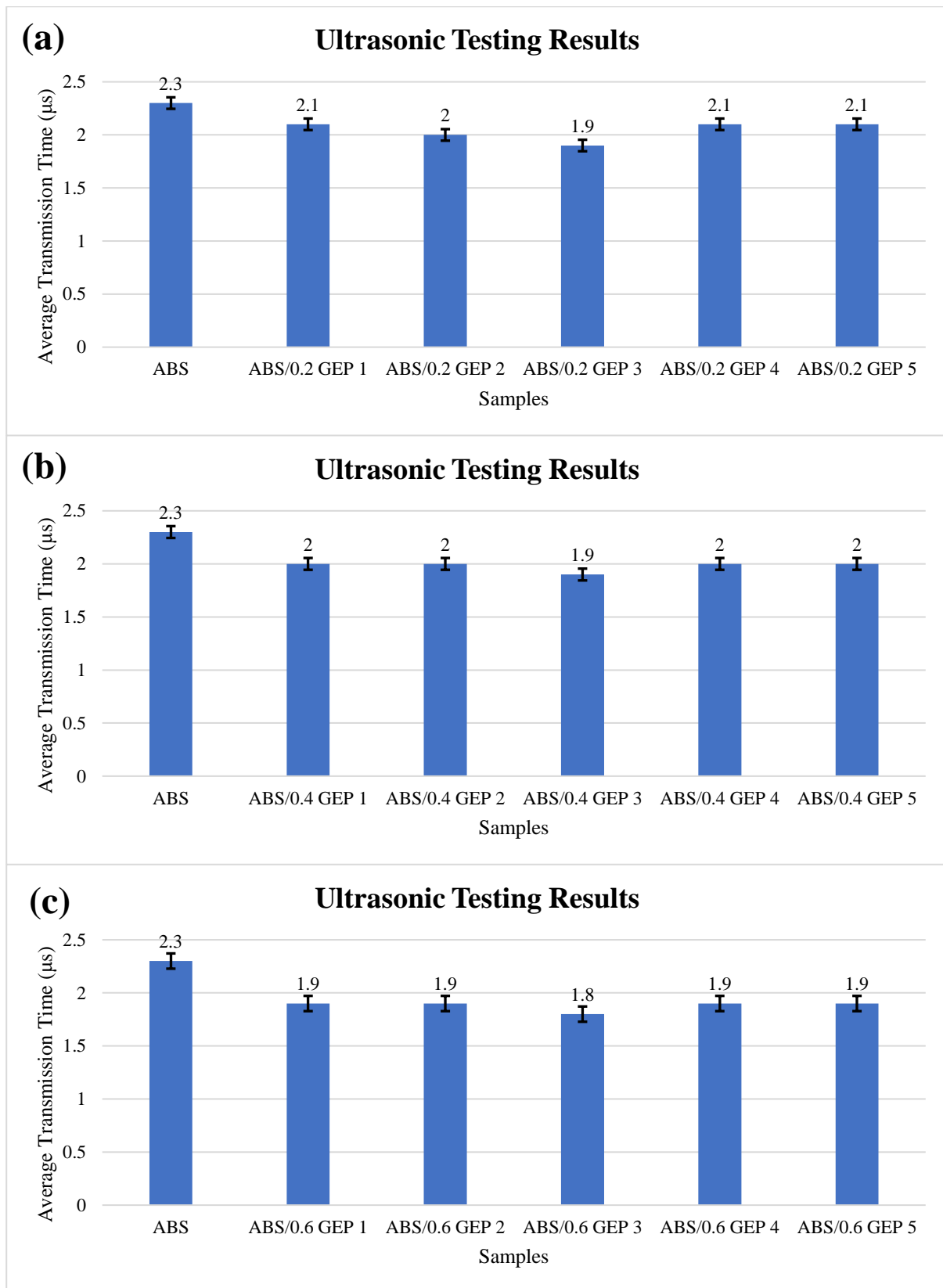


Figure 8. Ultrasonic testing results: (a) ABS/0.2 GEP composites with ABS; (b) ABS/0.4 GEP composites with ABS; (c) ABS/0.6 GEP composites with ABS.

ABS/0.2 GEP composites showed varied transmission times with the lowest value observed as 1.9 μ s for three-layered ABS/0.2 GEP composites. The double-layered ABS/0.2 GEP composites showed a transmission time of 2.0 μ s and the highest transmission time of 2.1 μ s was observed for ABS/0.2 GEP 1, ABS/0.2 GEP 4, and ABS/0.2 GEP 5 composites, as shown in Figure 8a. On the other hand, ABS/0.4GEP composites showed transmission time of 2.0 μ s for the first two layers whereas the 3-layered ABS/0.4 GEP composites showed the lowest transmission time of 1.9 μ s. The transmission times increased for ABS/0.4 GEP with 4 and 5 layers, as shown Figure 8b. Among all the composites, ABS/0.6 GEP composites showed consistent transmission times. The first two layers showed transmission time of 1.9 μ s, with the lowest being observed for 3-layered ABS/0.6 GEP composites. Both 4 and 5 layers of ABS/0.6 GEP composites showed transmission times of 1.9 μ s (Figure 8c). The results show that adding TA material to ABS reduced voids and gaps, resulting in stronger bonding between the layers.

3.4. Tensile Testing

The tensile testing was carried out on the manufactured samples to investigate the bonding integrity and fracture load values of CPM-manufactured plastic composites. All the samples exhibited brittle failure, meaning that the samples did not show any plastic deformation or necking before the fracture. ABS showed an average load value of 1050 N. The composites manufactured from CPM showed a significant increase to their tensile strength when compared to ABS. The maximum load values and stress-strain curve for ABS/GCHP composites were plotted for comparison in Figure 9. Single-layered ABS/GCHP composites showed an average load value of 1205 N with an increase of 14.7% when compared to ABS. The double-layered samples showed an average load value of 1273.5 N with an increase of 21.2%. The highest average load value of 1334 N was observed for triple-layered ABS/GCHP composites with an increase of 27%. ABS/GCHP 4 and ABS/GCHP 5 showed an average load value of 1244 N and 1216.25 N, respectively. It is evident in Figure 9 that an increase was observed until layer 3 and then a decrease from 4 layers onwards. It was observed that the tensile strength decreased after the addition of three layers of TA materials to ABS. This highlights that the maximum number of TA material layers that can be added to a 4 mm sample is three. After the addition of four layers, the average load started to decrease.

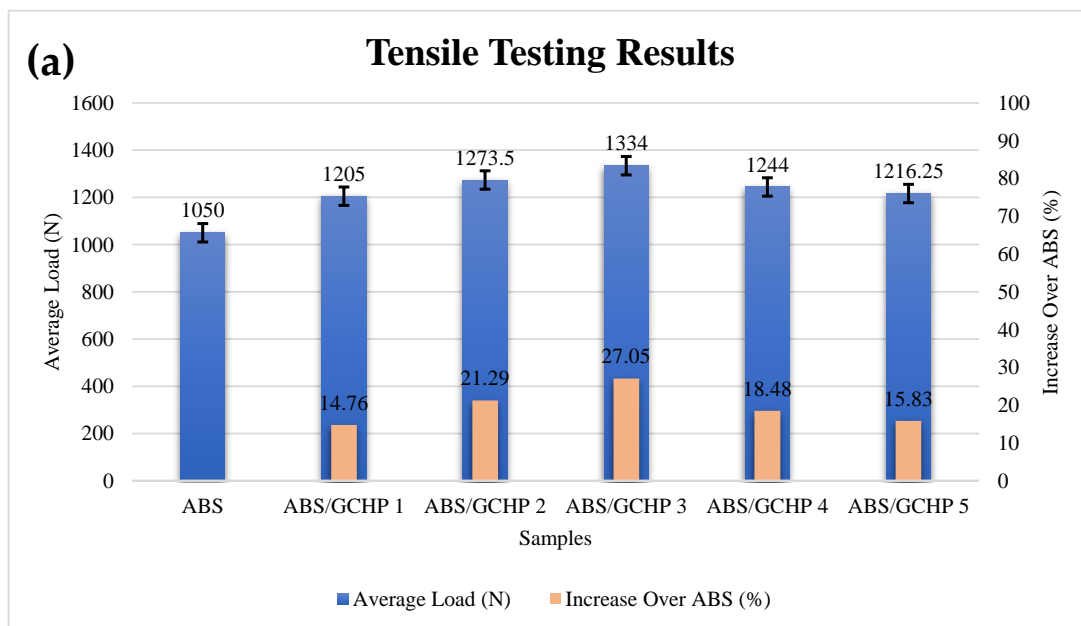


Figure 9. Cont.

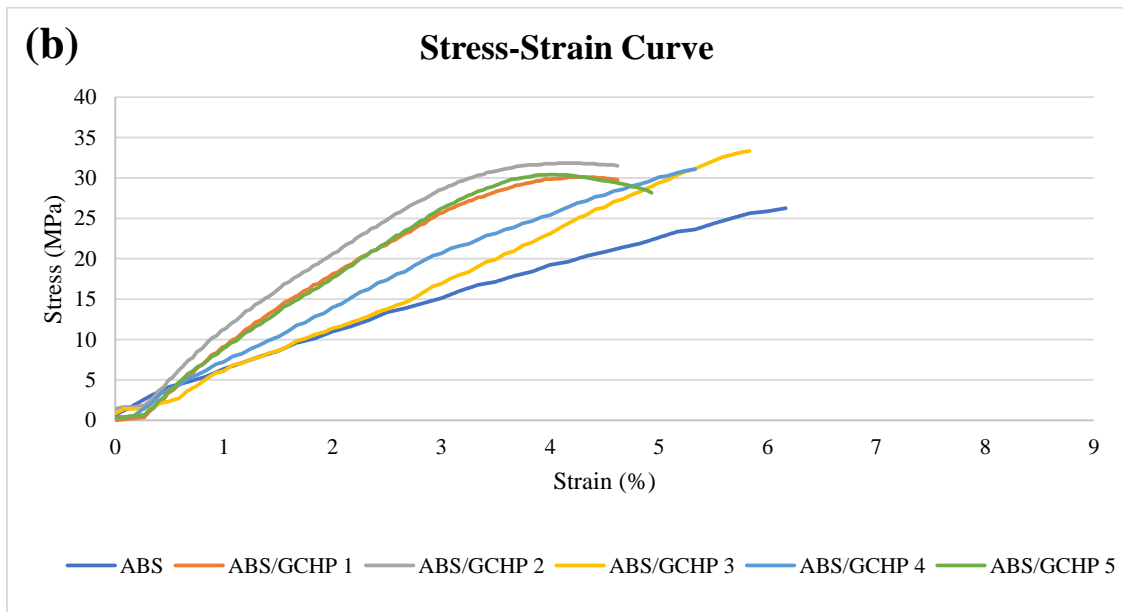


Figure 9. Comparative tensile test results for ABS/GCHP composites: (a) results from tensile testing with standard deviation as error bars; (b) stress-strain curve.

Furthermore, a correlation could be observed between the tensile results and ultrasonic testing, as shown in Figure 10. The average transmission time decreased as the tensile strength increased, indicating a significant correlation between the two test results. This is due to samples with higher strength being more densely packed and having better layer adhesion, allowing sound waves to travel through them quickly [15,26,45,46,61]. The lowest transmission time of 1.9 μs and highest average load value of 1334N was observed for three-layered ABS/GCHP samples. This showed the presence of strong bonding in the three-layered samples.

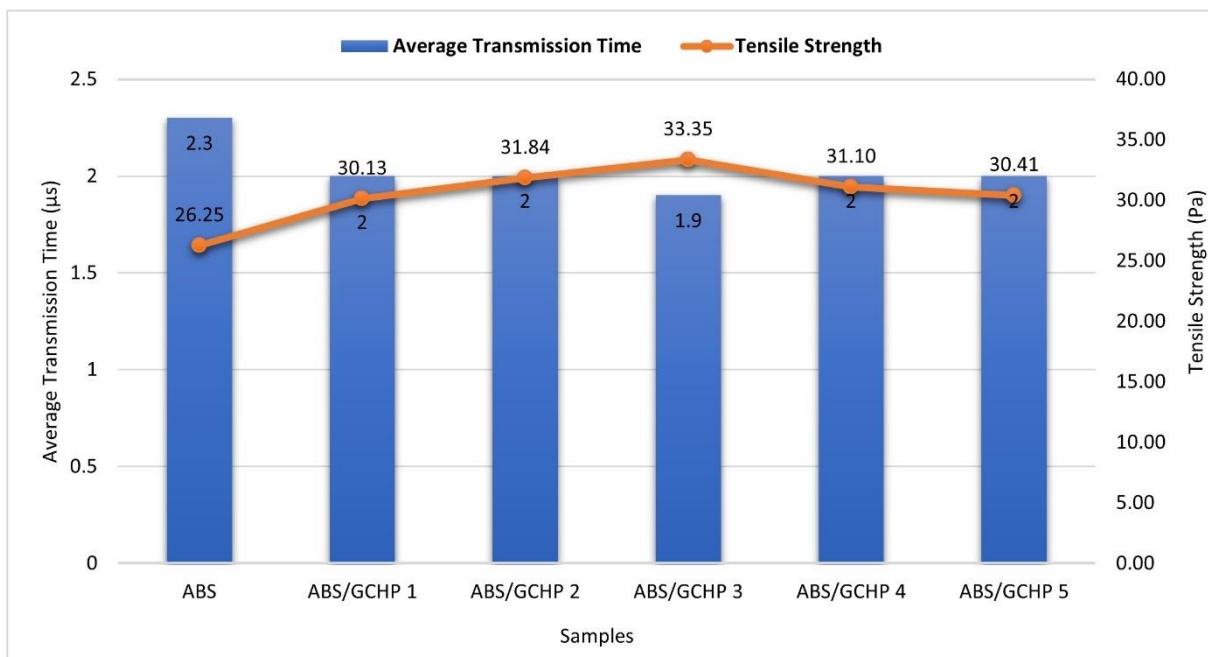


Figure 10. Correlation between average transmission times and tensile strength for ABS/GCHP composites.

The results for ABS/HCE composites were plotted for comparison in Figure 11. A single-layered ABS/HCE samples showed an average load value of 1135 N with an increase of 8.1% when compared to ABS. ABS/HCE 2 showed an average load value of 1154 N with an increase of 9.9%. Like ABS/GCHP composites, the highest average load value was observed for three-layered composites. The three-layered ABS/HCE composites showed an average load value of 1246 N with an increase of 18.6% when compared to ABS. The 4- and 5-layered ABS/HCE composites showed a decrease from 3-layered samples, but still an increase of 11.8% and 8.19% when compared to ABS. This can be further supported through the ultrasonic testing, where a lower transmission time was observed for three-layered ABS/GCHP and ABS/HCE composites. The presence of voids was minimal for three-layered composites, thereby demonstrating a strong bonding between TA and ABS due to the presence of heat throughout the manufacturing process. The heat relieves the internal stresses in the ABS layers and allows the TA materials to cure in a timely manner, thereby creating a stronger bond [46].

Figure 12 shows the correlation between average transmission times and tensile strength for ABS/HCE composites. It can be seen that the samples with lower transmission time of sound waves showed increased tensile strength. This is because the samples with higher transmission times had voids and gaps with weaker bonding of ABS and HCE.

ABS/HCE 3 samples showed higher tensile strength, meaning that the layers were tightly packed and possessed better adhesion, thus allowing the sound waves to travel faster through the solid, resulting in lower transmission times. The lowest transmission time of 1.9 μ s and high average load value of 1246 N was observed for three-layered ABS/HCE samples. All the other samples showed slightly increased transmission time of 2.0 μ s, indicating the presence of voids.

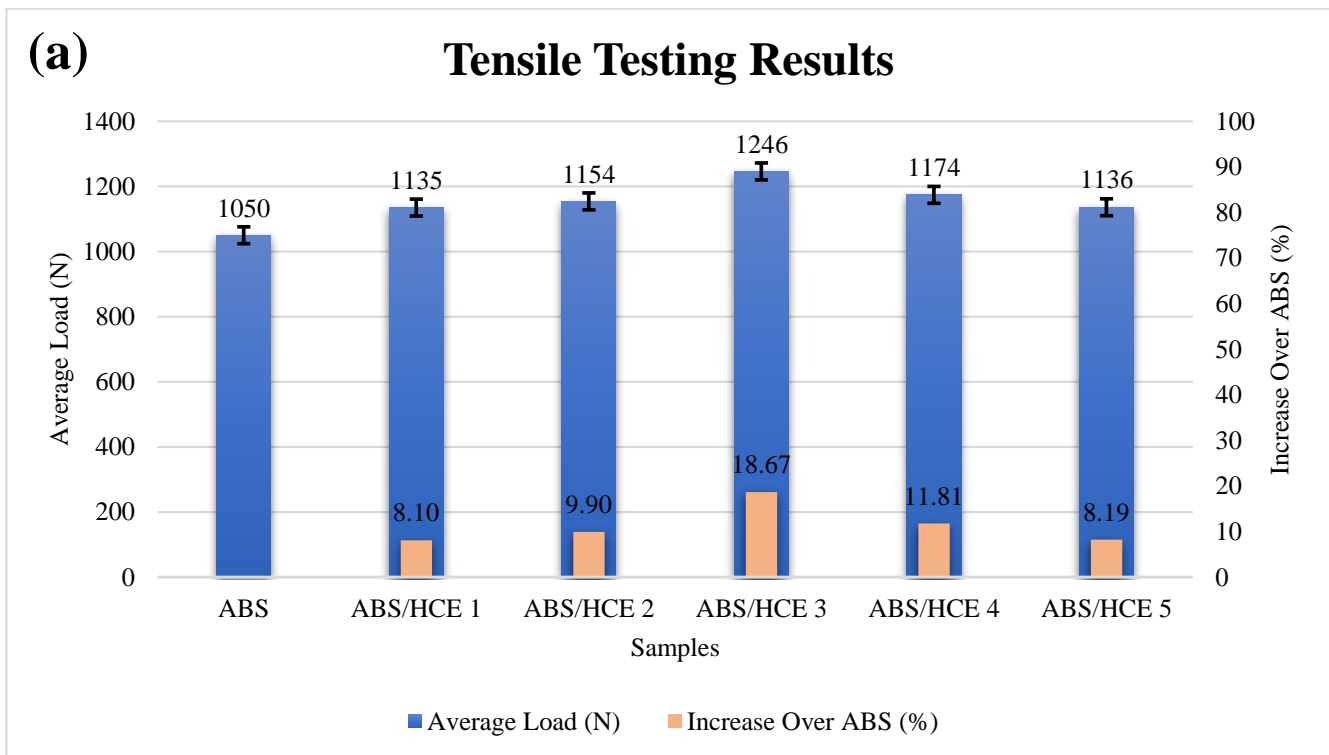


Figure 11. Cont.

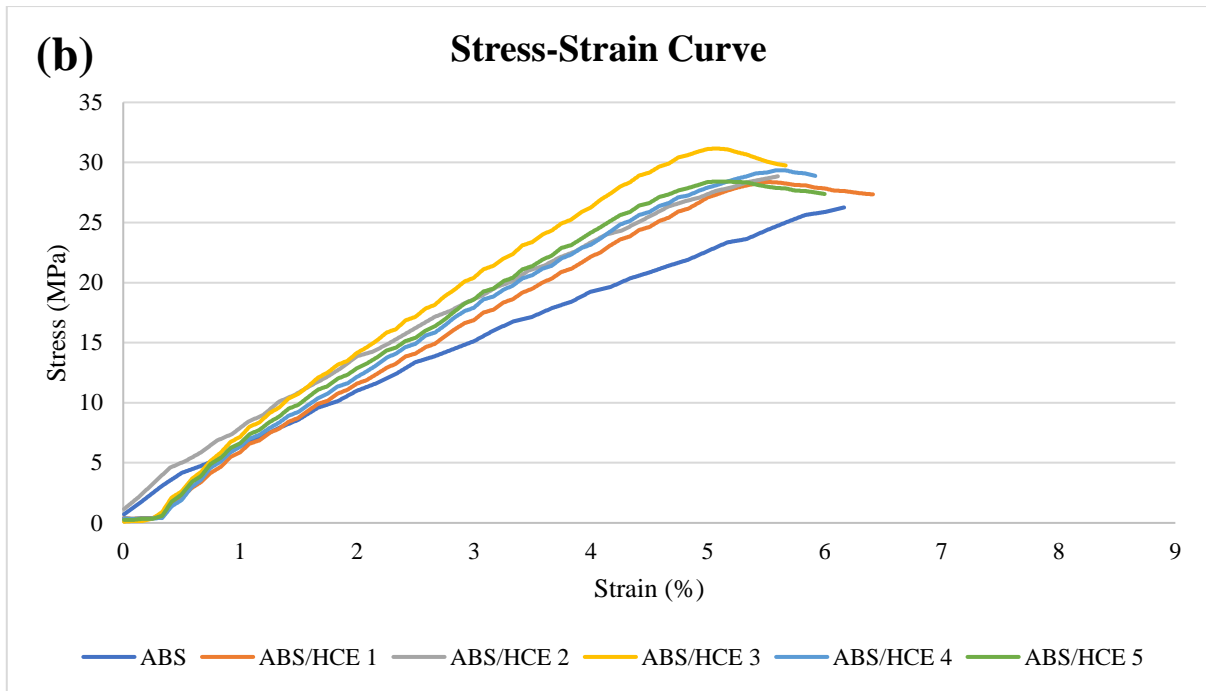


Figure 11. Comparative tensile test results for ABS/HCE composites: (a) results from tensile testing with standard deviation as error bars; (b) stress-strain curve.

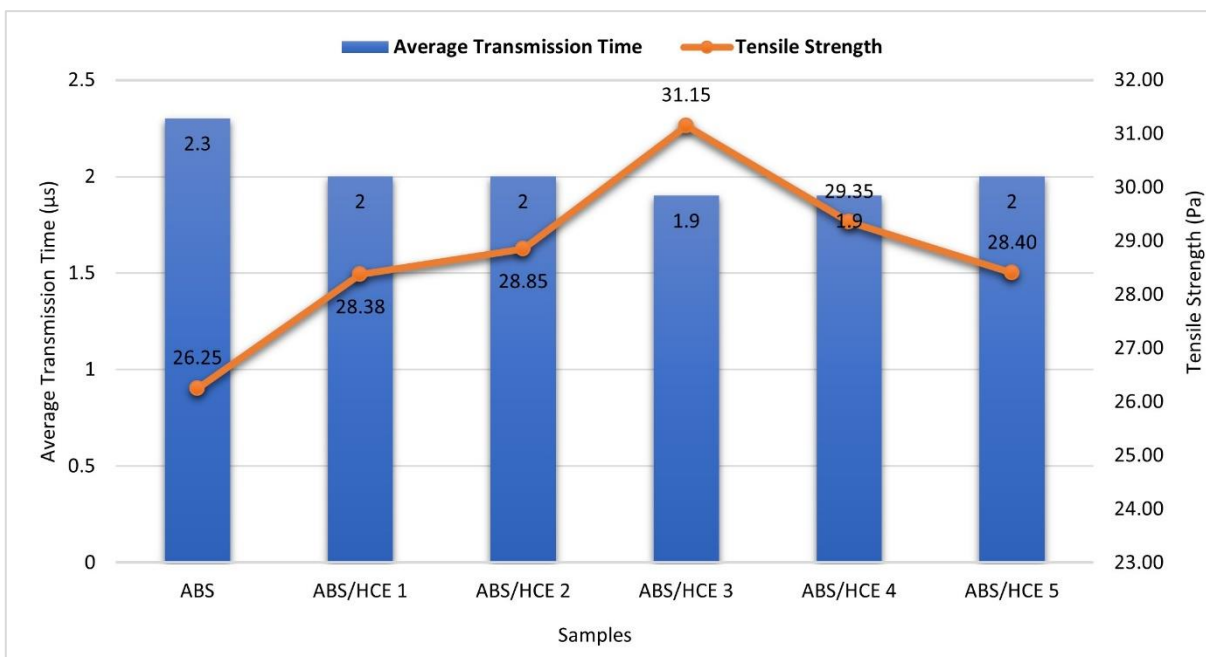


Figure 12. Correlation between average transmission times and tensile strength for ABS/HCE composites.

ABS/GEP composites were manufactured with three different contents of GNPs (0.2 wt.%, 0.4 wt.%, and 0.6 wt.%) mixed with HCE. The addition of GNPs to the HCE significantly increased the tensile strength. Figure 13 shows the stress-strain curve and maximum load values of ABS/0.2 GEP composites. A single-layered ABS/0.2 GEP samples showed an average load value of 1145 N with an increase of 9% when compared to ABS, whereas the double-layered ABS/0.2 GEP samples showed an average load value of 1195 N with an increase of 13.8%. Like ABS/GCHP and ABS/HCE composites, the highest value was observed for three-layered composites, as shown in Figure 13a. The three-layered

ABS/0.2 GEP samples showed the highest average load value of 1281 N with an increase of 22%. For those with 4 and 5 layers, the values started to go down but an increase of 13.3% and 12.8% was observed when compared to ABS.

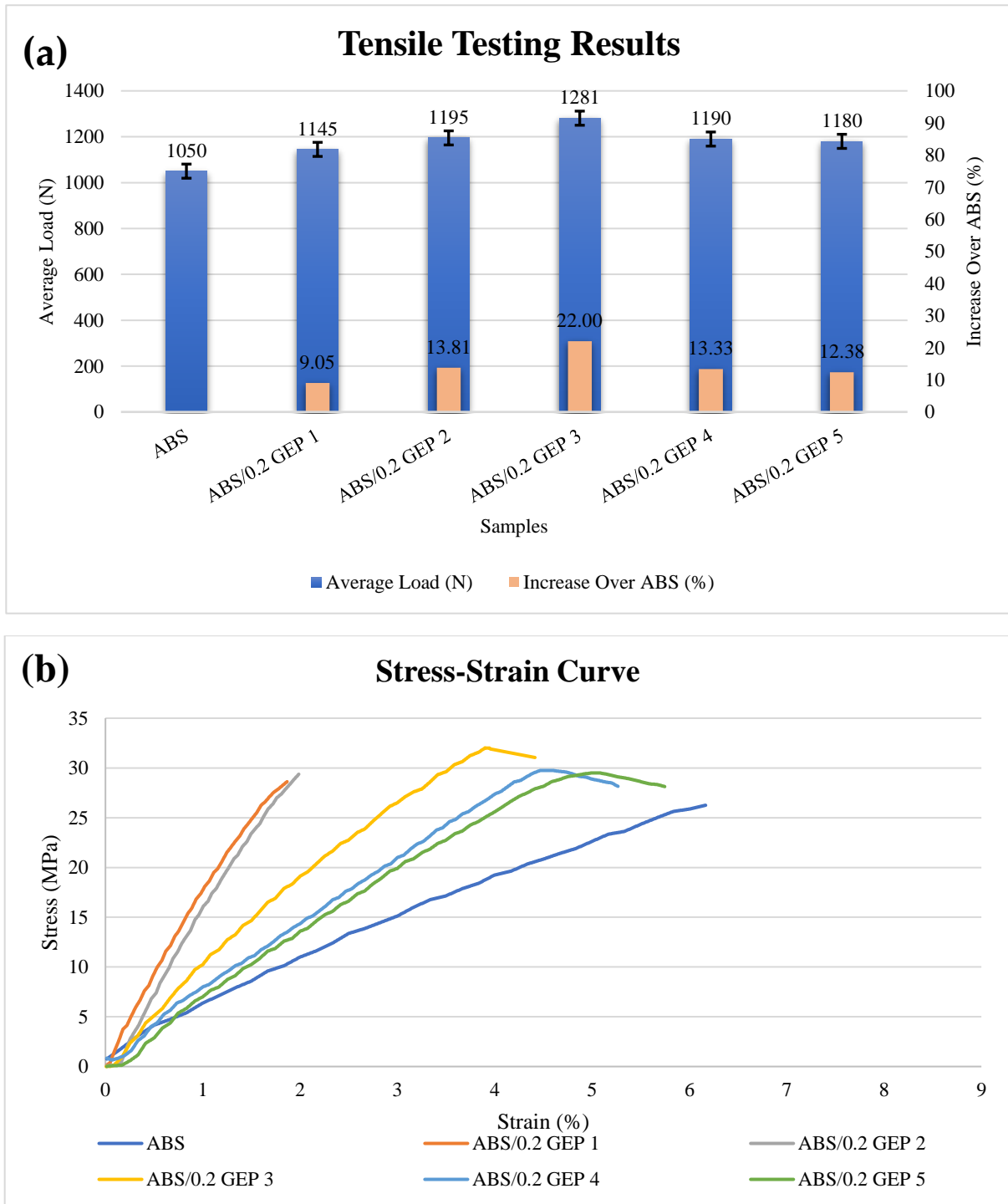


Figure 13. Comparative tensile test results for ABS/0.2 GEP composites: (a) results from tensile testing with standard deviation as error bars; (b) stress-strain curve.

It is evident that a lower transmission of 1.9 μ s was observed for three-layered ABS/0.2 GEP samples, which resulted in a higher average load value. Figure 14 shows the correlation between average transmission times and tensile strength for ABS and ABS/0.2 GEP composites. The ultrasonic results for ABS/0.2 GEP showed varied trans-

mission times across all the 5 layers, but the values started to go down from 2 layers onwards. The tensile strength increased by 7.1% from double-layered (29.88 MPa) to triple-layered (32.03 MPa) ABS/0.2 GEP composites. This indicates presence of minimal voids in three-layered samples, resulting in higher tensile strength of the samples.

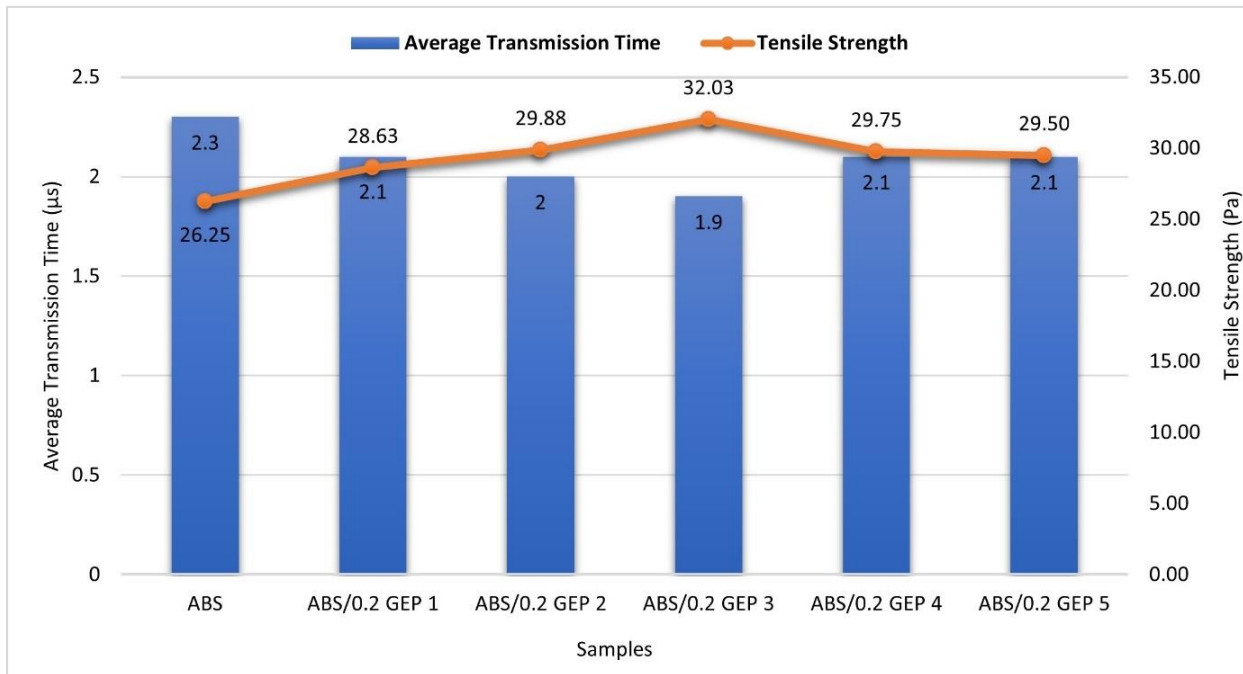


Figure 14. Correlation between average transmission times and tensile strength for ABS/0.2 GEP composites.

The results for ABS/0.4 GEP composites were plotted for comparison in Figure 15. The single-layered ABS/0.4 GEP composites showed an average load value of 1230 N with an increase of 17.14% when compared to ABS. On the other hand, the double-layered ABS/0.4 GEP samples showed an average load value of 1273.50 N with an increase of 21.29%. The highest average load value of 1347 N was observed for three-layered ABS/0.4 GEP composites with an increase of 28.29%.

Figure 16 shows the correlation between average transmission times and tensile strength for ABS and ABS/0.4 GEP composites. Like other CPM plastic composites, the average load value started to decrease for those with 4 and 5 layers. The decrease was shown to be at −3.58% and −5.43% for ABS/0.4 GEP 4- and 5-layer composites when compared to 3-layered samples.

However, those with both 4 and 5 layers showed an increase of 24.71% and 22.86% when compared to ABS, as shown in Figure 15a. The ultrasonic results also showed a lower transmission time of 1.9 μs for three-layered ABS/0.4 GEP samples. The value started increasing for those with 4 and 5 layers to 2.0 μs. The increase in transmission time means layers were not closely bonded and there were voids and airgaps affecting the weld zones between the printed layers [15,26,45,46,61]. The results for ABS/0.6 GEP composites have been plotted for comparison in Figure 17. A single-layered ABS/0.6 GEP samples showed an average load value of 1354.5 N with an increase of 29% when compared to ABS. The two-layered ABS/0.6 GEP samples showed an average load value of 1386 N with an increase of 32%. Like other CPM composites, three-layered samples showed higher tensile strength, which was identified as the optimal number for the addition of TA material. ABS/0.6 GEP three-layered composites showed the highest value of 1397 N with an increase of 33%. This was the highest average value observed among all the tested composites.

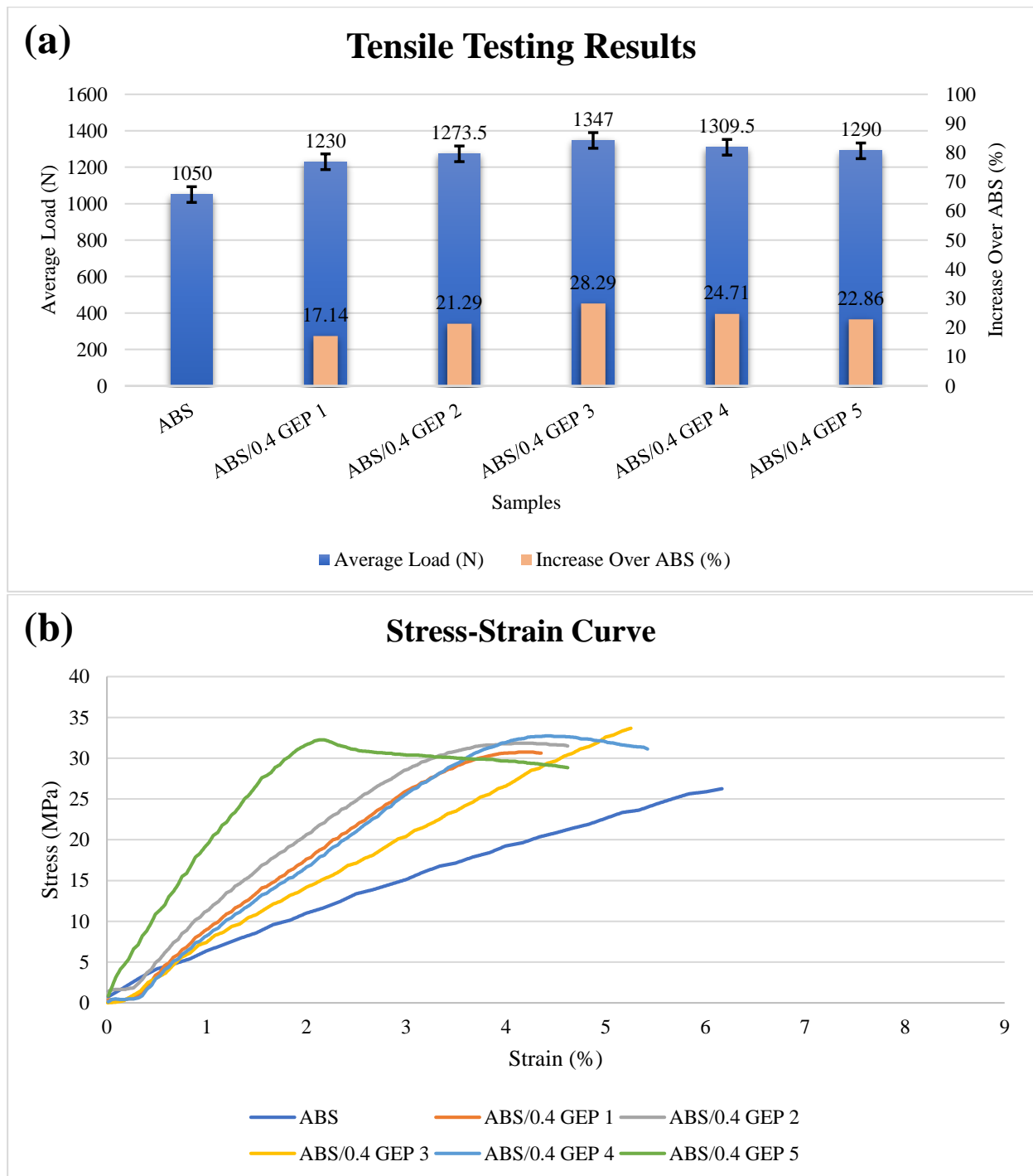


Figure 15. Comparative tensile test results for ABS/0.4 GEP composites: (a) results from tensile testing with standard deviation as error bars; (b) stress-strain curve.

It was also evident that an increase in average load value was observed for every +0.2 wt.% increase in GEP concoction. After the optimal number of TA material layers, the tensile strength started to deteriorate and resulted in lower values. It is to be noted that the 4- and 5-layered ABS/0.6 GEP composites showed an increase of 28% and 25.2% when compared to ABS. Figure 18 shows the correlation between average transmission times and tensile strength for ABS and ABS/0.4 GEP composites.

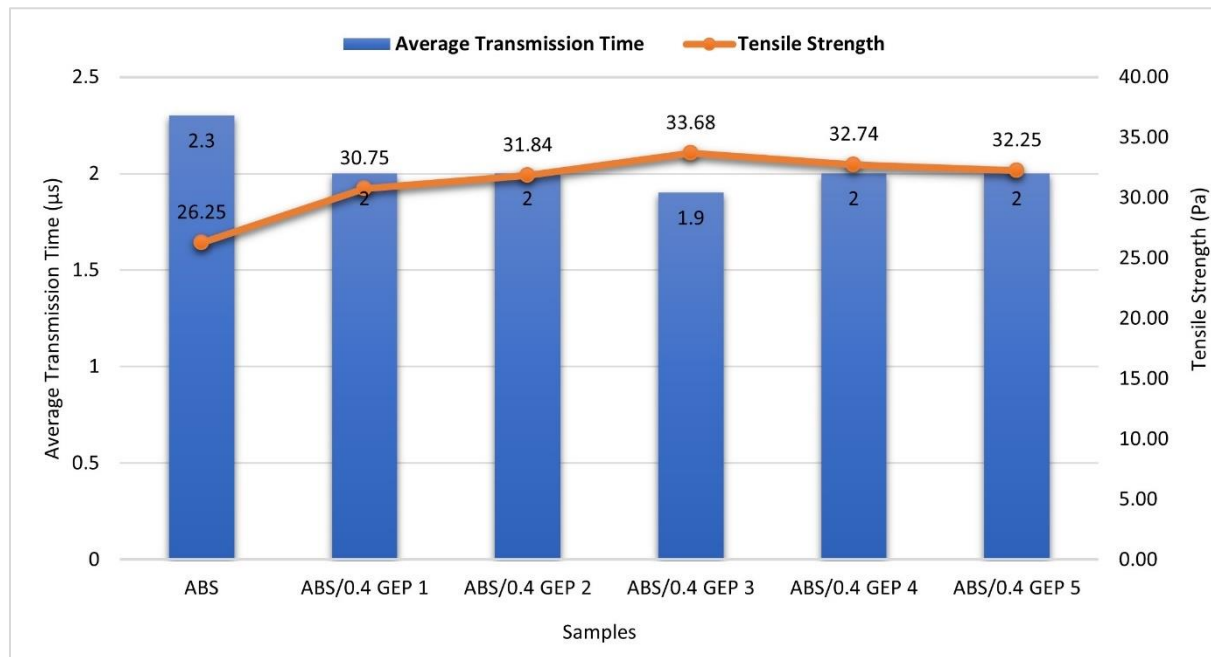


Figure 16. Correlation between average transmission times and tensile strength for ABS/0.4 GEP composites.

The bonding mechanism was strengthened because a covalent bond formed between ABS and thermally activated materials. A chemical bond known as a covalent bond involves the exchanging of electrons between atoms to create electron pairs. Polymer structures typically have long chains of covalently bonded carbon and hydrogen atoms in various arrangements. Covalent bonding mostly occurs in non-metallic elements. Epoxy is an organic compound made of carbon chains linked to additional elements such as hydrogen, oxygen, or nitrogen. The covalent bond used to maintain this connection between the elements involves sharing two electrons. Graphene material also shares a covalent bond, as each carbon atom is covalently bonded to three other carbon atoms. The thermally activated material adheres to the ABS plastic because the electrons are clouded internally and shared between the layers and form strong covalent bond (sp² hybridization).

To further substantiate the results of the composites made by CPM, the results were also compared to those in the literature. Tambrallimath et al. [28] developed a polymer nanocomposite filament to manufacture parts using fused deposition modeling (FDM). The composites filaments were obtained using the melt blend and extrusion technique of polycarbonate (PC) and acrylonitrile butadiene styrene (ABS) with graphene nanoparticles (GNPs) in different proportions (0.2 wt.%, 0.4 wt.%, 0.6 wt.%, and 0.8 wt.%). The process involved several preprocessing techniques such as drying the PC and ABS pellets for 4 h to remove moisture and then compounding them together at different temperature to obtain the composite filament. This results in a longer lead time to achieve the composite filament. In the case of CPM, the highest tensile strength was obtained when three layers of TA materials were added to ABS, as this is the optimal number of layers that can be added to a 4 mm tensile test sample. The highest tensile strengths obtained from CPM plastic composites were plotted for comparison with PC–ABS–graphene composites (addition of GNPs up to 0.6 wt.%), as shown in Figure 19. The PC–ABS showed a tensile strength of 22.33 MPa. The addition of GNPs increased the tensile strength up to 28.64 MPa for PC–ABS with 0.6 wt.%. On the other hand, the highest tensile strength of 34.93 MPa was observed for three-layered ABS/0.6 GEP composites. ABS/GCHP and ABS/HCE composites showed an increase of 16.4% and 8.7% when compared to composites manufactured through the composite filament manufactured by Tambrallimath et al. [28] using the FDM process. ABS/GEP (0.2 wt.%, 0.4 wt.%, and 0.6 wt.%) composites showed an increase of 11.8%, 17.8%

and 21.9% when compared to PC-ABS + 0.6 wt.% GNP composites. This clearly highlights the effectiveness of the CPM process to produce high-strength composites without the use of time-consuming pre- or postprocessing.

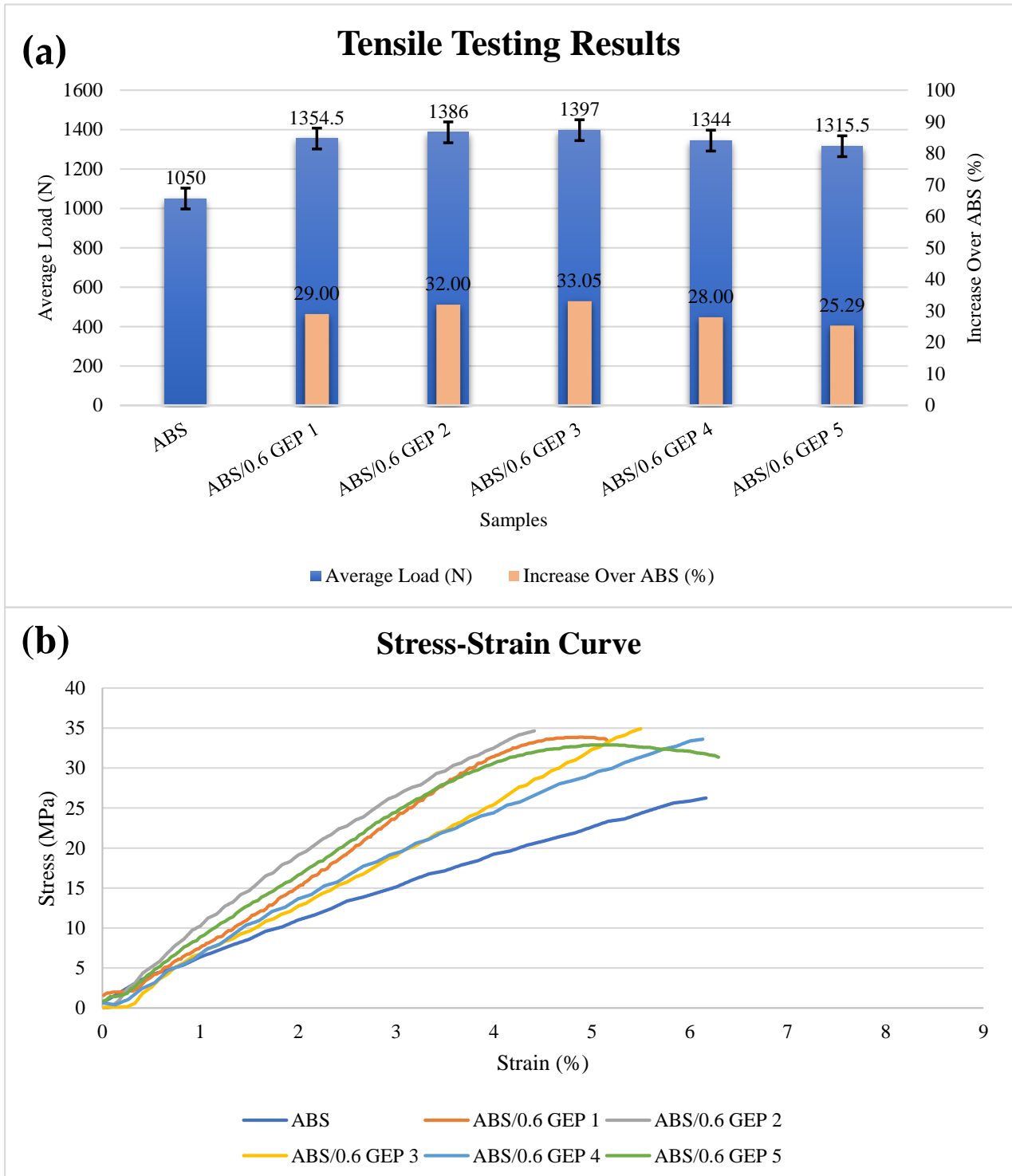


Figure 17. Comparative tensile test results for ABS/0.6 GEP composites: (a) results from tensile testing with standard deviation as error bars; (b) stress-strain curve.

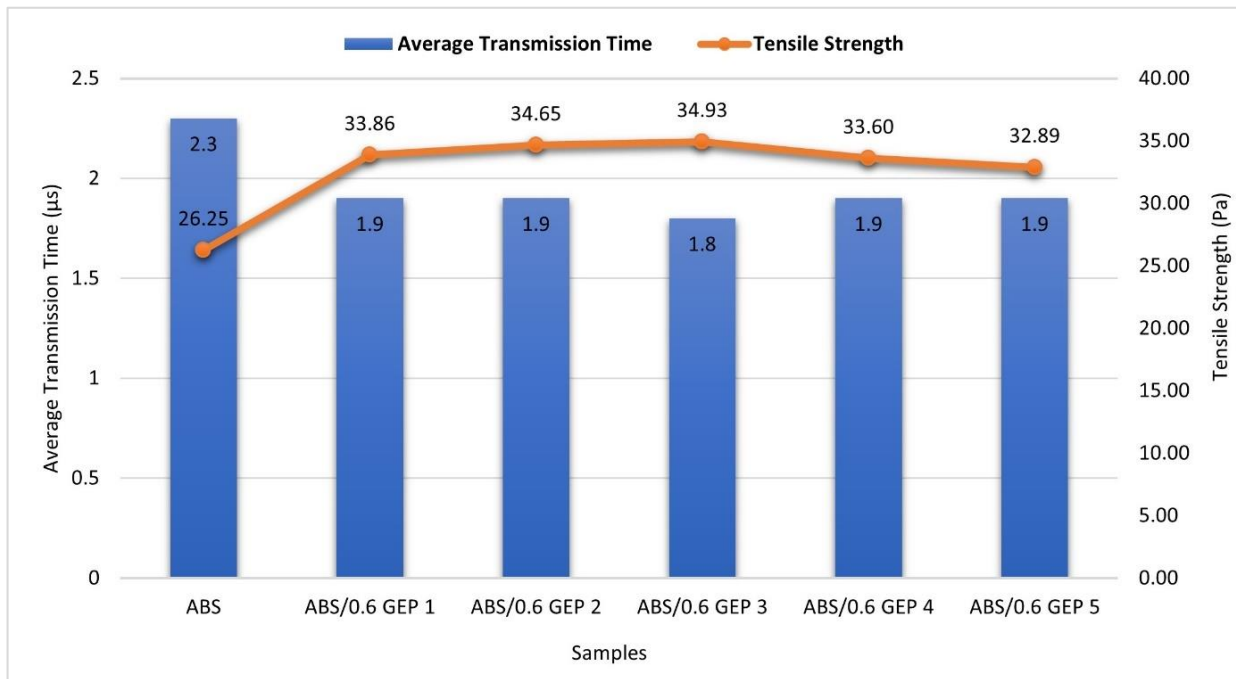


Figure 18. Correlation between average transmission times and tensile strength for ABS/0.6 GEP composites.

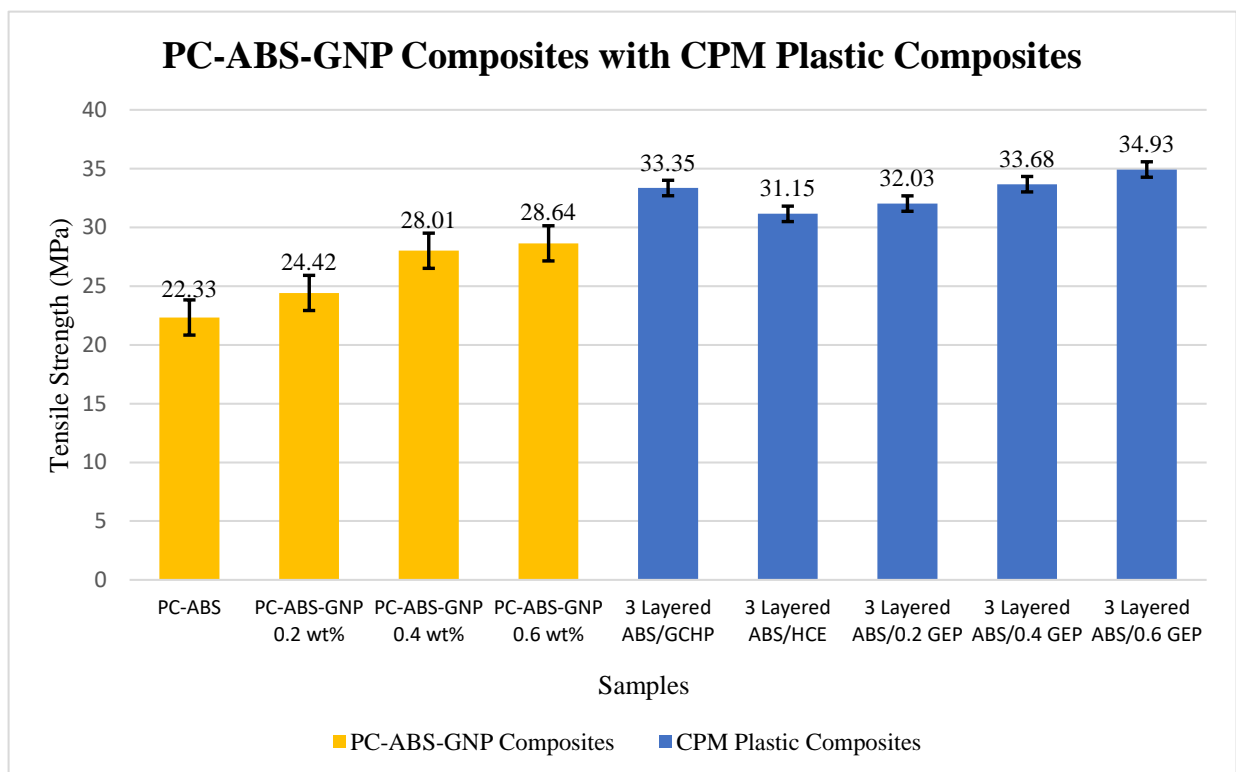


Figure 19. Results of PC-ABS-GNP composites compared with those of CPM plastic composites.

3.5. Hardness Testing

Hardness testing was conducted to determine the hardness of plastic composites manufactured by the CPM process. ABS showed a hardness value of 64.5 HD. A single layer of TA material was added to ABS at three different completions, i.e., 70%, 80%, 90%.

It is evident from the results that CPM plastic composites showed a significant increase in hardness when compared to ABS. The reason for adding TA material at three different completions (70%, 80%, 90%) was to make the indenter reach the TA material layer and analyze its reaction forces.

A single layer of GCHP added to ABS at 70% showed 73 HD with 13.1% increase to its hardness value and ABS/GCHP 80% showed 75 HD with an increase of 16.2%. ABS/GCHP 90% composites showed a hardness value of 77 HD with an increase of 19.3% from ABS. Figure 20 shows the hardness results of ABS/GCHP composites compared to those of ABS.

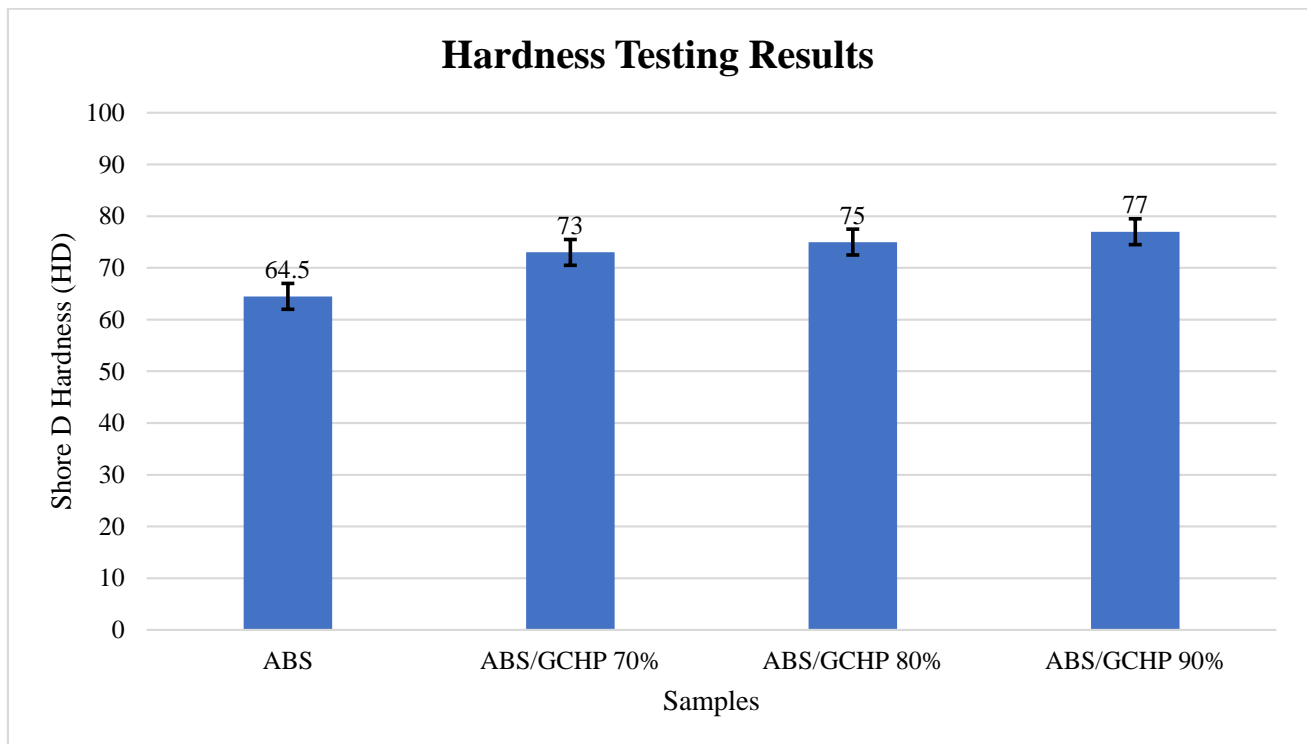


Figure 20. Hardness testing results for ABS/GCHP composites with ABS.

The hardness value increased when the TA material was layer added closer to the surface [46]. A single layer of HCE added at 70% to ABS/HCE showed 72 HD with an 11.6% increase to its hardness value and ABS/HCE 80% showed a slight increase (15.50%) of 74.5 HD compared to ABS. ABS/HCE 90% composites showed a hardness value of 76 HD with an increase of 17.8% from ABS, as shown in Figure 21.

Figure 22 shows the hardness results of ABS/GEP composites with ABS. A single layer of GEP with 0.2 wt.% GNPs added at 70% to ABS showed 75 HD, an increase of 16.28% compared to ABS. ABS/0.2 80% showed slight increase of 77 HD. ABS/0.2 GEP 90% composites showed a hardness value of 79 HD with an increase of 22.4% from ABS, as shown in Figure 22a. A single layer of GEP (0.4 wt.% GNPs) added at 70% to ABS showed 79 HD, an increase of 22.4% compared to ABS. ABS/0.4 80% showed a slight increase of 80 HD. ABS/0.4 GEP 90% composites showed a hardness value of 81.5 HD with an increase of 26.36% from ABS, as shown in Figure 22b. Similarly, a single layer of GEP (0.6 wt.% GNPs) added at 70% to ABS showed 80 HD, an increase of 24% compared to ABS. ABS/0.6 80% showed a hardness value of 82 HD, and the highest hardness value of 84 HD was observed for ABS/0.6 GEP composite when a TA material layer was added at 90% completion. This is an increase of 30.23% when compared to FFF-manufactured ABS, as shown in Figure 22c.

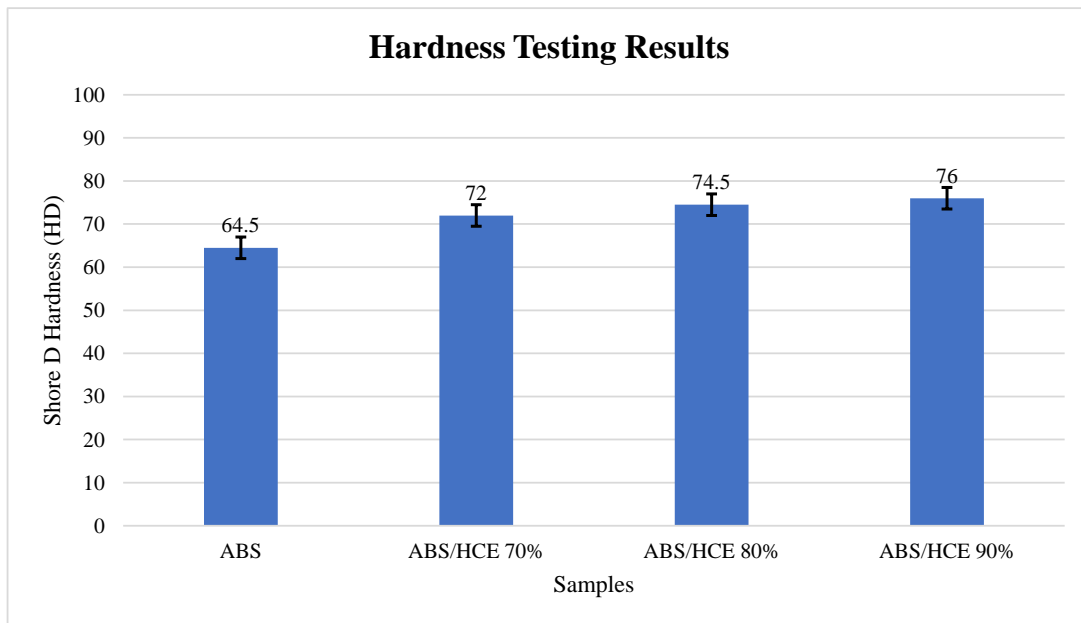


Figure 21. Hardness testing results for ABS/HCE composites with ABS.

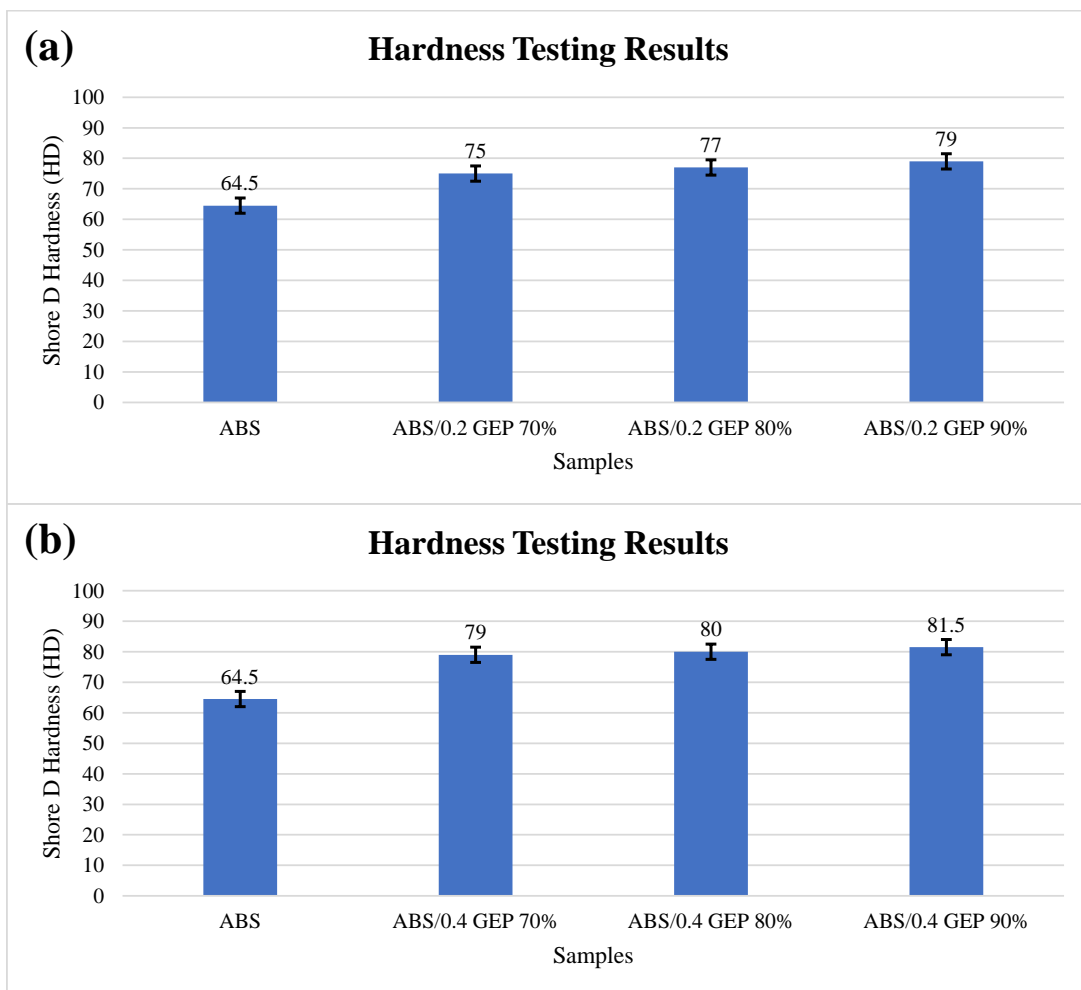


Figure 22. Cont.

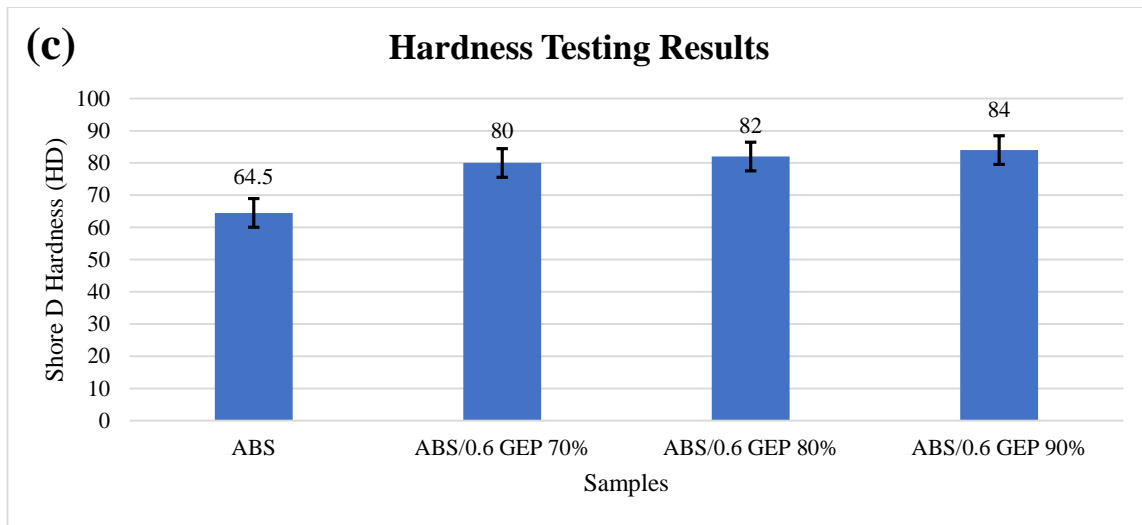


Figure 22. Hardness testing results: (a) ABS/0.2 GEP composites with ABS; (b) ABS/0.4 GEP composites with ABS; (c) ABS/0.6 GEP composites with ABS.

3.6. Three-Point Flexural Testing

Three-point flexural testing is used to determine a material’s flex or bending properties. The samples were manufactured and tested according to BS EN ISO 178:2019 [53]. Figure 23 shows the three-point flexural testing results for all the samples. ABS exhibited brittle failure and fractured with a clean break, as expected. The composites manufactured from CPM also exhibited brittle failure and did not exhibit any striations. The composites manufactured by CPM showed a significant increase in their flexural strength when compared to ABS. Flexural strength of 119 MPa was observed for ABS. The TA material was interlaced at three different intervals (single-, double-, and triple-layered composites) for the flexural test samples, as shown in Table 4.

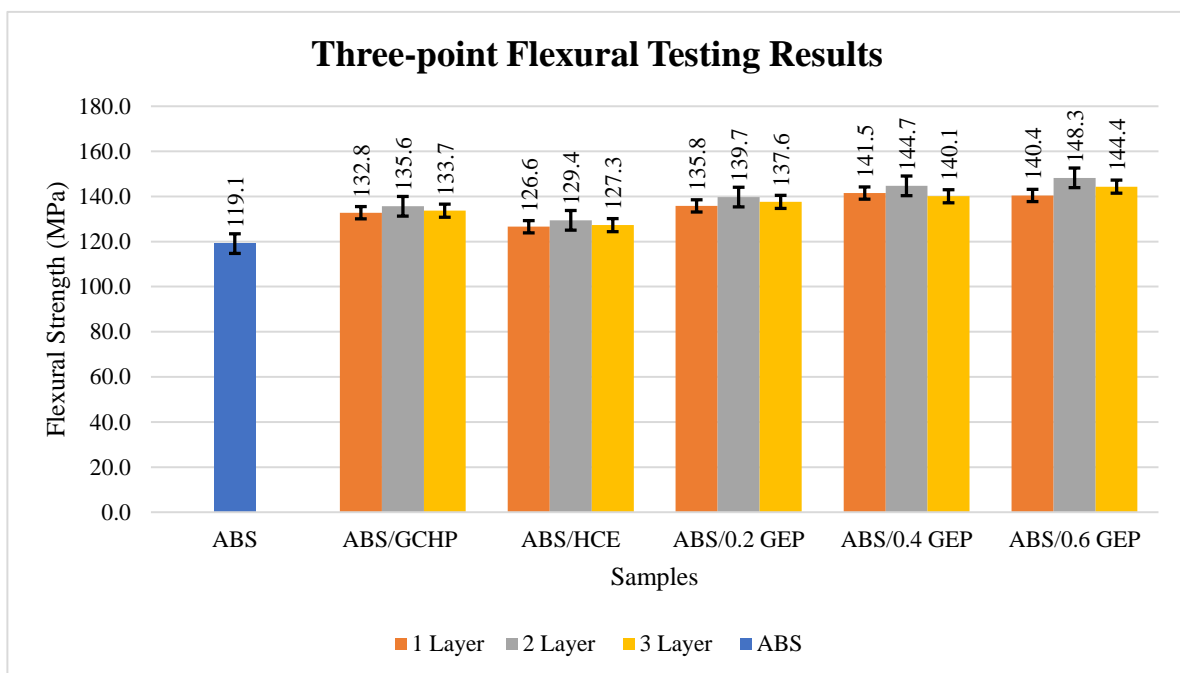


Figure 23. Three-point flexural testing results of ABS-based plastic composites with ABS.

ABS/GCHP composites showed a significant increase in their flexural strength compared to ABS. The single-layered ABS/GCHP samples showed a flexural strength of 132.8 MPa, which was an increase of 11.4% over ABS. The double-layered ABS/GCHP samples showed a flexural strength of 135.6 MPa (an increase of 13.8%). However, the three-layered ABS/GCHP composites exhibited a decrease from double-layered composites, but still an increase of 12.2% compared to ABS. The same phenomenon was observed for ABS/HCE composites. The single-layered ABS/HCE samples showed a flexural strength of 126.5 MPa (an increase of 6.2%) whereas the double-layered ABS/HCE samples showed a flexural strength of 129.4 MPa (an increase of 8.6%). The three-layered ABS/HCE composites exhibited a decrease from double-layered composites but an increase of 6.8% compared to ABS. Both graphene–carbon hybrid paste and heat cure epoxy are commercially available TA materials and they showed a similar increase pattern in their flexural strength.

Three different GEP concoctions were prepared using GNPs (0.2 wt.%, 0.4 wt.%, and 0.6 wt.%) and interlaced with ABS to manufacture flexural test samples. The composites manufactured using GEP followed a similar pattern to the commercial TA materials. The single-layered ABS/0.2 GEP samples showed a flexural strength of 135.8 MPa (an increase of 14%) and the double-layered ABS/0.2 GEP samples showed a flexural strength of 139.7 MPa (an increase of 17.3%). The three-layered ABS/0.2 GEP composites exhibited a decrease from double-layered composites but with an increase of 15.5% compared to ABS. The single-layered ABS/0.4 GEP samples showed a flexural strength of 141.5 MPa (an increase of 18.8%) whereas the double-layered ABS/0.4 GEP samples showed a flexural strength of 144.7 MPa (an increase of 21.4%). The three-layered ABS/0.4 GEP composites exhibited a decrease from double-layered composites but with an increase of 17.6% compared to ABS. The single-layered ABS/0.6 GEP samples showed a flexural strength of 140.4 MPa (an increase of 17.9%) and the double-layered ABS/0.6 GEP samples showed a flexural strength of 148.27 MPa (an increase of 24.4%). The three-layered ABS/0.6 GEP composites exhibited a decrease from double-layered composites but with an increase of 21.1% compared to ABS. The results were consistent and show the effectiveness of the CPM process.

4. Conclusions

In this study, CPM was employed to manufacture plastic-based composites using various TA materials (graphene–carbon hybrid paste, heat cure epoxy paste, and graphene epoxy paste). CPM is a new additive manufacturing process developed to produce plastic-based composites in a cost- and time-effective manner. Commonly available ABS was interlaced with TA materials at different intervals to assess whether adding more TA materials improved mechanical properties. Testing samples were manufactured and tested according to British and international standards to demonstrate the effectiveness of CPM in terms of manufacturing high-quality plastic composites with customized properties. The following conclusions were drawn from this research work:

1. The measurement of mass was carried out on the manufactured samples to investigate the effect of adding multiple layers of TA materials to 4 mm tensile samples. Commercially available ABS manufactured using the FFF process showed a mass of 9.78 g with a percentage difference of -2.2% . The composites manufactured using the CPM process showed consistent mass for all the samples. Furthermore, the composites showed a 0.2 g increase in their mass for every single layer addition of TA material. The highest mass value of 9.88 g was observed for five-layered composites with a percentage difference of -1.2% , which is within the tolerance of actual mass (10 g) generated in Ultimaker Cura software during slicing. It is evident from the results that the parts manufactured by CPM are not adversely affected by the addition of TA material to ABS and it enhanced the accuracy of the overall mass. The mass of the desired part can be adjusted based on the product requirements, thus making the process versatile to produce bespoke parts with customised properties.
2. Dimensional analysis showed that CPM is able to manufacture plastic composites in a consistent manner with minimal inaccuracies. An increase of 0.1 mm in total

thickness (z-axis) was observed for every single layer addition of TA materials, and these tolerances can be taken into consideration by designers based on the product requirements. The consistent deposition of TA material improved the dimensional accuracy of the final product, thereby enhancing the mechanical properties, which cannot be achieved in FFF-manufactured parts.

3. Ultrasonic testing was conducted to assess whether the addition of TA material to ABS reduced the voids/porosity and air gaps common in FFF-manufactured parts. All the composites showed lower transmission times when compared to commercially available ABS. The presence of voids and air gaps was reduced for 1-, 2-, and 3-layered plastic composites, resulting in lower transmission times and strong layer bonding. The transmission times slightly increased for 4- and 5-layered composites, but they were lower than those of commercially available ABS. The results show that the addition of multiple layers of TA material to ABS did not adversely affect the deposited layers. Furthermore, the composites showed consistent transmission times for all the different TA materials. It was also evident that the voids, internal stresses, and air gaps were reduced due to the nature of CPM process, as parts were built under constant temperature for curing TA materials. This helped in minimizing these defects and achieved an upward trend of tensile strength as well.
4. Tensile testing showed consistent increase in fracture load values for all the samples. A total of five layers of three different TA materials were added to 4 mm tensile samples at different intervals. The tensile strength kept increasing for every single layer addition of TA materials. However, the increase was observed for up to 3 layers and then decreased for 4- and 5-layered composites. This phenomenon was observed for all the TA materials. The highest tensile strength of 34.9 MPa was observed for ABS/0.6 GEP three-layered composites and this was an increase of 33% over commercially available ABS. This shows that the addition of more layers deteriorates the properties, highlighting the optimal number of TA material layers that can be added to a product. All the 3-layered plastic composites showed increasing tensile strength until layer 3 and then a reduction for 4- and 5-layered composites. The addition of one TA material layer should be restricted to 1 mm (i.e., a 4 mm thickness should have only three layers of TA material). This indicates that the maximum number of TA material layers that can be added to a product is limited by the product's overall thickness.
5. Hardness testing showed positive results for all the plastic composites manufactured by CPM. A single layer of TA material was added at different intervals of build (70%, 80%, and 90%) to analyze its reaction force. The results showed increased hardness value when the TA material layer was added closer to the surface at 90% completion. The highest hardness value of 84 HD was observed for ABS/0.6 GEP with an increase of 30.2% over commercial ABS (64.5 HD).
6. Three-point flexural tests showed that the addition of TA material layers increased flexural strength, correlating with the tensile test results. A total of three layers of TA material were added to the flexural samples (3 mm thickness) at different intervals. The flexural strength kept increasing for every single layer addition of TA materials. However, the increase was observed for up to 2 layers and then decreased for 3-layered samples. This phenomenon was observed for all the TA materials. The highest flexural strength of 148.2 MPa was observed for ABS/0.6 GEP three-layered composites and this was an increase of 24.4% over commercially available ABS.

Author Contributions: Conceptualization, R.B. and J.B.; methodology, R.B. and J.B.; validation, R.B., J.B. and H.S.; formal analysis, R.B. and J.B.; investigation, R.B.; resources, R.B. and H.S.; data curation, R.B.; writing—original draft preparation, R.B.; writing—review and editing, R.B. and J.B.; visualization, R.B.; project administration, R.B. All authors have read and agreed to the published version of the manuscript.

Funding: This research was funded by European Regional Development Fund (ERDF), as part of the KEEP+ Programme (KEEP+ ref: 635) between Anglia Ruskin University and Transporter Engineering Limited.

Data Availability Statement: The data used in this research work can be made available upon request.

Conflicts of Interest: The authors declare no conflict of interest.

References

1. Salifu, S.; Desai, D.; Ogunbiyi, O.; Mwale, K. Recent development in the additive manufacturing of polymer-based composites for automotive structures—A review. *Int. J. Adv. Manuf. Technol.* **2022**, *119*, 6877–6891. [[CrossRef](#)]
2. Zhuo, P.; Li, S.; Ashcroft, I.A.; Jones, A.I. Material extrusion additive manufacturing of continuous fibre reinforced polymer matrix composites: A review and outlook. *Compos. Part B Eng.* **2021**, *224*, 109143. [[CrossRef](#)]
3. Yuan, S.; Li, S.; Zhu, J.; Tang, Y. Additive manufacturing of polymeric composites from material processing to structural design. *Compos. Part B Eng.* **2021**, *219*, 108903. [[CrossRef](#)]
4. Zagorski, M.; Sofronov, Y.; Ivanova, D.; Dimova, K. Investigation of different FDM/FFF 3D printing methods for improving the surface quality of 3D printed parts. *AIP Conf. Proc.* **2022**, *2449*, 060001. [[CrossRef](#)]
5. Sola, A. Materials Requirements in Fused Filament Fabrication: A Framework for the Design of Next-Generation 3D Printable Thermoplastics and Composites. *Macromol. Mater. Eng.* **2022**, *307*, 2200197. [[CrossRef](#)]
6. Valino, A.D.; Dizon, J.R.C.; Espera, A.H., Jr.; Chen, Q.; Messman, J.; Advincula, R.C. Advances in 3D printing of thermoplastic polymer composites and nanocomposites. *Prog. Polym. Sci.* **2019**, *98*, 101162. [[CrossRef](#)]
7. Dickson, A.N.; Abourayana, H.M.; Dowling, D.P. 3D printing of fibre-reinforced thermoplastic composites using fused filament fabrication—A review. *Polymers* **2020**, *12*, 2188. [[CrossRef](#)]
8. Roy, R.; Mukhopadhyay, A. Tribological studies of 3D printed ABS and PLA plastic parts. *Mater. Today Proc.* **2021**, *41*, 856–862. [[CrossRef](#)]
9. Djokicj, J.; Tuteski, O.; Doncheva, E.; Hadjieva, B. Experimental investigation on mechanical properties of FFF parts using different materials. *Procedia Struct. Integr.* **2022**, *41*, 670–679. [[CrossRef](#)]
10. Selvam, A.; Mayilswamy, S.; Whenish, R.; Naresh, K.; Shanmugam, V.; Das, O. Multi-objective optimization and prediction of surface roughness and printing time in FFF printed ABS polymer. *Sci. Rep.* **2022**, *12*, 16887. [[CrossRef](#)]
11. Ninikas, K.; Kechagias, J.; Fountas, N.A.; Vaxevanidis, N.M. A study of Fused Filament Fabrication process efficiency: ABS vs PLA materials. *IOP Conf. Ser. Mater. Sci. Eng.* **2022**, *1235*, 012007. [[CrossRef](#)]
12. La Gala, A.; Ceretti, D.V.; Fiorio, R.; Cardon, L.; D'hooge, D.R. Comparing pellet-and filament-based additive manufacturing with conventional processing for ABS and PLA parts. *J. Appl. Polym. Sci.* **2022**, *139*, e53089. [[CrossRef](#)]
13. Shaik, Y.P.; Schuster, J.; Shaik, A. A Scientific Review on Various Pellet Extruders Used in 3D Printing FDM Processes. *Open Access Libr. J.* **2021**, *8*, 1–19. [[CrossRef](#)]
14. Butt, J.; Mebrahtu, H.; Shirvani, H. Numerical and experimental analysis of product development by composite metal foil manufacturing. *Int. J. Rapid Manuf.* **2018**, *7*, 59–82. [[CrossRef](#)]
15. Butt, J.; Bhaskar, R.; Mohaghegh, V. Investigating the effects of extrusion temperatures and material extrusion rates on FFF-printed thermoplastics. *Int. J. Adv. Manuf. Technol.* **2021**, *117*, 2679–2699. [[CrossRef](#)]
16. Butt, J.; Bhaskar, R.; Mohaghegh, V. Investigating the Effects of Ironing Parameters on the Dimensional Accuracy, Surface Roughness, and Hardness of FFF-Printed Thermoplastics. *J. Compos. Sci.* **2022**, *6*, 121. [[CrossRef](#)]
17. Butt, J.; Bhaskar, R.; Mohaghegh, V. Investigating the Influence of Material Extrusion Rates and Line Widths on FFF-Printed Graphene-Enhanced PLA. *J. Manuf. Mater. Process.* **2022**, *6*, 57. [[CrossRef](#)]
18. Butt, J.; Bhaskar, R.; Mohaghegh, V. Analysing the effects of layer heights and line widths on FFF-printed thermoplastics. *Int. J. Adv. Manuf. Technol.* **2022**, *121*, 7383–7411. [[CrossRef](#)]
19. Mohan, V.B.; Lau, K.T.; Hui, D.; Bhattacharyya, D. Graphene-based materials and their composites: A review on production, applications and product limitations. *Compos. Part B Eng.* **2018**, *142*, 200–220. [[CrossRef](#)]
20. Gao, J. Production of multiple material parts using a desktop 3D printer. In *Advances in Manufacturing Technology XXXI, Proceedings of the 15th International Conference on Manufacturing Research, Incorporating the 32nd National Conference on Manufacturing Research, London, UK, 5–7 September 2017*; IOS Press: Amsterdam, The Netherlands, 2017; p. 148. [[CrossRef](#)]
21. Kottasamy, A.; Samykano, M.; Kadirgama, K.; Rahman, M.; Noor, M.M. Experimental investigation and prediction model for mechanical properties of copper-reinforced polylactic acid composites (Cu-PLA) using FDM-based 3D printing technique. *Int. J. Adv. Manuf. Technol.* **2022**, *119*, 5211–5232. [[CrossRef](#)]
22. Lebedev, S.M.; Gefle, O.S.; Amitov, E.T.; Zhuravlev, D.V.; Berchuk, D.Y.; Mikutskiy, E.A. Mechanical properties of PLA-based composites for fused deposition modeling technology. *Int. J. Adv. Manuf. Technol.* **2018**, *97*, 511–518. [[CrossRef](#)]
23. Hwang, S.; Reyes, E.I.; Moon, K.S.; Rumpf, R.C.; Kim, N.S. Thermo-mechanical characterization of metal/polymer composite filaments and printing parameter study for fused deposition modeling in the 3D printing process. *J. Electron. Mater.* **2015**, *44*, 771–777. [[CrossRef](#)]
24. Heidari-Rarani, M.; Rafiee-Afarani, M.; Zahedi, A.M. Mechanical characterization of FDM 3D printing of continuous carbon fiber reinforced PLA composites. *Compos. Part B Eng.* **2019**, *175*, 107147. [[CrossRef](#)]

25. Butt, J.; Shirvani, H. Experimental analysis of metal/plastic composites made by a new hybrid method. *Addit. Manuf.* **2018**, *22*, 216–222. [[CrossRef](#)]
26. Butt, J.; Hewavidana, Y.; Mohaghegh, V.; Sadeghi-Esfahlani, S.; Shirvani, H. Hybrid manufacturing and experimental testing of glass fiber enhanced thermoplastic composites. *J. Manuf. Mater. Process.* **2019**, *3*, 96. [[CrossRef](#)]
27. Butt, J.; Oxford, P.; Sadeghi-Esfahlani, S.; Ghorabian, M.; Shirvani, H. Hybrid manufacturing and mechanical characterization of Cu/PLA composites. *Arab. J. Sci. Eng.* **2020**, *45*, 9339–9356. [[CrossRef](#)]
28. Tambrallimath, V.; Keshavamurthy, R.; Bavan, S.D.; Patil, A.Y.; Yunus Khan, T.M.; Badruddin, I.A.; Kamangar, S. Mechanical properties of PC-ABS-based graphene-reinforced polymer nanocomposites fabricated by FDM process. *Polymers* **2021**, *13*, 2951. [[CrossRef](#)]
29. Dul, S.; Fambri, L.; Pegoretti, A. Fused deposition modelling with ABS–graphene nanocomposites. *Compos. Part A Appl. Sci. Manuf.* **2016**, *85*, 181–191. [[CrossRef](#)]
30. Vidakis, N.; Maniadi, A.; Petousis, M.; Vamvakaki, M.; Kenanakis, G.; Koudoumas, E. Mechanical and electrical properties investigation of 3D-printed acrylonitrile–butadiene–styrene graphene and carbon nanocomposites. *J. Mater. Eng. Perform.* **2020**, *29*, 1909–1918. [[CrossRef](#)]
31. Aumnate, C.; Pongwisuthiruchte, A.; Pattananuwat, P.; Potiyaraj, P. Fabrication of ABS/graphene oxide composite filament for fused filament fabrication (FFF) 3D printing. *Adv. Mater. Sci. Eng.* **2018**, *2018*, 2830437. [[CrossRef](#)]
32. Sun, J.; Ji, J.; Chen, Z.; Liu, S.; Zhao, J. Epoxy resin composites with commercially available graphene: Toward high toughness and rigidity. *RSC Adv.* **2019**, *9*, 33147–33154. [[CrossRef](#)] [[PubMed](#)]
33. Hmeidat, N.S.; Kemp, J.W.; Compton, B.G. High-strength epoxy nanocomposites for 3D printing. *Compos. Sci. Technol.* **2018**, *160*, 9–20. [[CrossRef](#)]
34. Compton, B.G.; Lewis, J.A. 3D-printing of lightweight cellular composites. *Adv. Mater.* **2014**, *26*, 5930–5935. [[CrossRef](#)] [[PubMed](#)]
35. Bustillos, J.; Montero, D.; Nautiyal, P.; Loganathan, A.; Boesl, B.; Agarwal, A. Integration of graphene in poly (lactic) acid by 3D printing to develop creep and wear-resistant hierarchical nanocomposites. *Polym. Compos.* **2018**, *39*, 3877–3888. [[CrossRef](#)]
36. Dorigato, A.; Moretti, V.; Dul, S.; Unterberger, S.H.; Pegoretti, A. Electrically conductive nanocomposites for fused deposition modelling. *Synth. Met.* **2017**, *226*, 7–14. [[CrossRef](#)]
37. Jyoti, J.; Kumar, A.; Dhakate, S.R.; Singh, B.P. Dielectric and impedance properties of three dimension graphene oxide-carbon nanotube acrylonitrile butadiene styrene hybrid composites. *Polym. Test.* **2018**, *68*, 456–466. [[CrossRef](#)]
38. Sezer, H.K.; Eren, O. FDM 3D printing of MWCNT re-inforced ABS nano-composite parts with enhanced mechanical and electrical properties. *J. Manuf. Processes* **2019**, *37*, 339–347. [[CrossRef](#)]
39. Ning, F.; Cong, W.; Qiu, J.; Wei, J.; Wang, S. Additive manufacturing of carbon fiber reinforced thermoplastic composites using fused deposition modeling. *Compos. Part B Eng.* **2015**, *80*, 369–378. [[CrossRef](#)]
40. Castro-Casado, D. Chemical treatments to enhance surface quality of FFF manufactured parts: A systematic review. *Prog. Addit. Manuf.* **2021**, *6*, 307–319. [[CrossRef](#)]
41. de Bruijn, A.C.; Gómez-Gras, G.; Pérez, M.A. On the effect upon the surface finish and mechanical performance of ball burnishing process on fused filament fabricated parts. *Addit. Manuf.* **2021**, *46*, 102133. [[CrossRef](#)]
42. Rane, R.; Kulkarni, A.; Prajapati, H.; Taylor, R.; Jain, A.; Chen, V. Post-process effects of isothermal annealing and initially applied static uniaxial loading on the ultimate tensile strength of fused filament fabrication parts. *Materials* **2020**, *13*, 352. [[CrossRef](#)] [[PubMed](#)]
43. Arjun, P.; Bidhun, V.K.; Lenin, U.K.; Amritha, V.P.; Pazhamannil, R.V.; Govindan, P. Effects of process parameters and annealing on the tensile strength of 3D printed carbon fiber reinforced polylactic acid. *Mater. Today Proc.* **2022**, *62*, 7379–7384. [[CrossRef](#)]
44. Valvez, S.; Silva, A.P.; Reis, P.N.B.; Berto, F. Annealing effect on mechanical properties of 3D printed composites. *Procedia Struct. Integr.* **2022**, *37*, 738–745. [[CrossRef](#)]
45. Butt, J.; Bhaskar, R. Investigating the effects of annealing on the mechanical properties of FFF-printed thermoplastics. *J. Manuf. Mater. Process.* **2020**, *4*, 38. [[CrossRef](#)]
46. Bhaskar, R.; Butt, J.; Shirvani, H. Experimental Analysis of Plastic-Based Composites Made by Composite Plastic Manufacturing. *J. Compos. Sci.* **2022**, *6*, 127. [[CrossRef](#)]
47. 3D FilaPrint. Available online: <https://shop.3dfilaprint.com/abs-extrafill-sky-blue-175mm-3d-printer-filament-8226-p.asp> (accessed on 27 October 2022).
48. Dycotec Materials: DM-GRA-9100S. Available online: <https://www.dycotecmaterials.com/product/dm-gra-9100s/> (accessed on 27 October 2022).
49. Permabond Engineering Adhesives: Permabond ES566 Heat Cure Epoxy 320 mL Cartridge. Available online: <https://www.permabond.co.uk/product-page/es566-heat-cure-epoxy-1-x-320ml-cartridge> (accessed on 27 October 2022).
50. Nanografi: Graphene Nanoplatelet. Available online: <https://nanografi.com/graphene/graphene-nanoplatelets/> (accessed on 27 October 2022).
51. BS EN ISO 527-2:2012; Plastics—Determination of Tensile Properties—Part 2: Test Conditions for Moulding and Extrusion Plastics. British, European and International Standard: London, UK, 2012.
52. BS EN ISO 868:2003; Plastics and Ebonite—Determination of Indentation Hardness by Means of a Durometer (Shore Hardness). British, European and International Standard: London, UK, 2018.

53. BS EN ISO 178:2019; Plastics—Determination of Flexural Properties. British, European and International Standard: London, UK, 2011.
54. Ultimaker Cura: Advanced 3D Printing Software, Made Accessible. Available online: <https://ultimaker.com/software/ultimaker-cura> (accessed on 27 October 2022).
55. Vevor: Ultrasonic Homogenizer Sonicator Cell Disruptor Mixer 80w 500 uL-50 mL Capacity. Available online: <https://www.vevor.co.uk/s/ultrasonic-homogenizer-sonicator-cell-disruptor-mixer-80w-500ul-50ml-capacity> (accessed on 27 October 2022).
56. Seretis, G.V.; Theodorakopoulos, I.D.; Manolakos, D.E.; Provatidis, C.G. Effect of sonication on the mechanical response of graphene nanoplatelets/glass fabric/epoxy laminated nanocomposites. *Compos. Part B Eng.* **2018**, *147*, 33–41. [CrossRef]
57. Yu, H.; Hermann, S.; Schulz, S.E.; Gessner, T.; Dong, Z.; Li, W.J. Optimizing sonication parameters for dispersion of single-walled carbon nanotubes. *Chem. Phys.* **2012**, *408*, 11–16. [CrossRef]
58. Baig, Z.; Mamat, O.; Mustapha, M.; Mumtaz, A.; Munir, K.S.; Sarfraz, M. Investigation of tip sonication effects on structural quality of graphene nanoplatelets (GNPs) for superior solvent dispersion. *Ultrason. Sonochem.* **2018**, *45*, 133–149. [CrossRef]
59. Mwema, F.M.; Akinlabi, E.T.; Fatoba, O.S. Visual assessment of 3D printed elements: A practical quality assessment for home-made FDM products. *Mater. Today Proc.* **2020**, *26*, 1520–1525. [CrossRef]
60. Lu, Q.Y.; Wong, C.H. Applications of non-destructive testing techniques for post-process control of additively manufactured parts. *Virtual Phys. Prototyp.* **2017**, *12*, 301–321. [CrossRef]
61. Butt, J.; Bhaskar, R.; Mohaghegh, V. Non-Destructive and Destructive Testing to Analyse the Effects of Processing Parameters on the Tensile and Flexural Properties of FFF-Printed Graphene-Enhanced PLA. *J. Compos. Sci.* **2022**, *6*, 148. [CrossRef]
62. Proceq PUNDIT® PL-200. Available online: <https://www.screeningeagle.com/en/products/pundit-200> (accessed on 27 October 2022).
63. Teckoplus HHTK-37D Digital Shore D Hardness Tester Durometer 0~100 HD. Available online: <https://www.tekcoplus.com/products/hhtk-37d> (accessed on 27 October 2022).